



Gas turbine engine transient performance and heat transfer effect modelling: A comprehensive review, research challenges, and exploring the future

Yimin Yang ^{*}, Theoklis Nikolaidis, Soheil Safari, Pericles Pilidis

Centre for Propulsion and Thermal Power Engineering, School of Aerospace Transport and Manufacturing (SATM), Cranfield University, Cranfield, Bedfordshire MK43 0AL, UK

ARTICLE INFO

Keywords:

Gas turbine engine
Transient performance
Heat soakage effect
Tip clearance effect
Component characteristic map

ABSTRACT

Gas turbine transient simulation is an important tool in analysing engine performance during changes in operating conditions. This paper provides a comprehensive review of the development of gas turbine transient simulation, heat transfer effect on transient performance and transient simulation platforms over the past 70 years. The paper highlights the various methods used for gas turbine overall transient simulation, including white box approach, black box approach and numerical approach, and the development of models for heat transfer effects, including heat soakage, tip clearance, and component characteristic changes. Besides, the development of gas turbine transient simulation platforms has been included. Challenges that need to be addressed to achieve more accurate simulations are identified. For white and black box approaches, complex engine dynamics phenomena and heat transfer effects urge the development of methodologies. For the numerical approach, the high computational and geometry demand for the full-size gas turbine transient model slows the CFD application in gas turbine overall transient simulation. For heat transfer effect simulation, the increasing complexity of engine structures and cooling techniques urges the development of a more realistic heat soakage model. The paper suggests that the white box approach can benefit from a method that accurately models several thermal dynamics. The black box methodologies should consider the heat transfer effect during the modelling and training. And more attention should be paid to the full-size gas turbine transient model development. Additionally, the paper recommends the development of a more complete heat transfer model that includes axial clearance effects, detailed combustor heat transfer models, and advanced component maps.

1. Introduction

When the gas turbine works at steady-state conditions, all engine parameters are kept constant. However, when the engine needs to move from one working point to another, it will experience an alert in fuel flow, leading to a performance change [1]. This process is called the gas turbine transient process. This process can last a few seconds for an aeroengine or hours for a heavy-duty gas turbine. For aeroengines, especially civil aeroengines, transient performance is a critical safety index and an essential certification requirement (the Federal Aircraft Administration specifies a 5-second acceleration time from flight idle to 95% thrust) [2]. For heavy-duty gas turbines, the transient performance is a key index related to the economic benefit, as it can take several hours to reach full load from a cold start due to its heavy casing and disc.

Moreover, challenging targets have been set by the Advisory Council for Aviation Research and Innovation in Europe (ACARE) for civil aircraft emissions and noise in Flightpath 2050 initiative. These targets include reductions of 75% in CO₂, 90% in NO_x, and 65% in noise compared to the typical new aircraft in 2000 [3]. These ambitious targets cannot be achieved solely by novel component technology design, and advanced gas turbine transient performance analysis is a promising way to help achieve these targets.

Many historical surveys have been published to provide a mature insight into gas turbine transient performance [4–8], and two main categories have been included in the engine transient analysis: (1) Gas turbine performance analysis during transient operation and (2) Heat transfer effects on transient performance. For transient performance analysis, researchers have focused on the methodology development and the establishment of the gas turbine engine model. Two domain

* Corresponding author.

E-mail address: yimin.yang96@cranfield.ac.uk (Y. Yang).

Nomenclature:		
A	Area / Aspect ratio of the blade	RBF Radial basis function
<i>a</i>	Speed of sound / Expansion coefficient / Blade shape constant	RMSE Root mean square relative error
ACARE	Advisory council for aviation research and innovation in europe	RNN Recurrent neural networks
ANN	Artificial neural networks	RSM Replacement structure model
ATEST	Advanced turbine engine simulation technique	SP Surplus power
<i>b</i>	Hidden layer	SSM State-space model
CFD	Computational fluid dynamics	T Temperature
CMF	Constant mass flow	TP Turbine power
CNN	Convolutional neural networks	<i>u</i> Internal energy / Thermal growth
<i>Cp</i>	Specific heat	V Velocity
CP	Compressor power	Vol Component volume
D	Characteristic diameter	W Mass flow
E	Material Young's modulus	<i>w</i> Connection weight
F	the ratio of the heat transferred from the air to the work transferred from the air	X Distense
FEM	Finite element method	<i>x</i> Input of neural network
GSP	Gas turbine simulation program	<i>y</i> Output of neural network
<i>h</i>	Enthalpy / heat transfer coefficient	
HPC	High pressure compressor	
HTC	Heat transfer coefficient	
<i>I</i>	Polar moment of inertia	
<i>i</i>	Incidence angle	
ICV	Inter-component volume	
IMF	Imbalanced mass flow	
IRM	Impulse response model	
<i>k</i>	Dimensionless constant / Thermal conductivity	
L	Characteristic length	
LES	Large eddy simulation	
LHV	Fuel lower heating values	
LPM	Lumped parameter method	
<i>m</i>	Mass	
mGT	Micro gas turbine	
MLP	Multi-layer perceptron	
<i>N</i>	Engine spool rotational speed	
NARX	Non-linear autoregressive exogenous	
NN	Neural network	
NPSS	Numerical propulsion system simulation	
<i>P</i>	Pressure	
PCN	Corrected rotational speed	
PROOSIS	Propulsion object oriented simulation software	
PW	Pressure waves	
PWV	Pressure wave in volume	
<i>Q</i>	Quantity of heat	
<i>q</i>	Heat flow rate	
<i>R</i>	Gas constant	
<i>R_q</i>	Inlet/exit heat transfer ratio	
ΔR	Change in radius	
<i>r</i>	Radius	
		<i>Greek letters</i>
		θ Altitude temperature ratio
		δ Altitude pressure ratio
		η Efficiency
		Δt Time interval
		γ Ratio of specific heats
		φ Real-valued function
		τ Time constant
		ρ Density
		ω Angular velocity
		ν Material Poisson's ratio
		λ Nondimensionalized clearance
		β Mean air angle
		ψ Blade loading coefficient
		ϕ Flow coefficient
		ψ_{Ztip} Zweifel loading coefficient
		Δa_2 Deflection angle
		ϵ^* Designed deflection
		<i>Subscript</i>
		<i>ad</i> Adiabatic
		<i>DP</i> Design Point
		<i>f</i> Fuel
		<i>g</i> gas
		<i>i</i> <i>i</i> th number
		<i>in</i> Inlet station
		<i>m</i> metal
		<i>new</i> Current time interval
		<i>old</i> Last time interval
		<i>out</i> outlet station
		<i>s</i> static
		<i>t</i> Time / Total
		Δt time interval
		0 undisturbed gas in front of the wave

approaches are widely used: the white box approach and the black box approach [4,9]. The former refers to models that are physically based. The gas turbine is represented by several governing equations, and components such as the compressor and turbine are normally modelled as 0-D components. Those models can capture engine components parameters, including mass flow and gas temperature at component inlet and outlet, spool rotational speed, net thrust, and exhaust gas temperature. The latter represents the use of artificial neural networks (ANN) to simulate the transient performance. In this approach, dynamic equations, thermodynamic relationships, and energy balance are no longer

the governing points. Instead, the focus is on input and output data. The numerical approach also plays an important role. However, compared with white and black box approach, the application on gas turbine transient performance is fewer. For the heat transfer effects, it was detected due to the mismatch between simulation results and experimental results [10]. These effects include the heat soakage effect, tip clearance effect and component characteristic change effect. They are caused by the heat exchange between the gas flow and the engine components and will lead to an impact on engine transient performance.

This paper aims to provide a comprehensive review of recent

progress and developments related to gas turbine overall transient performance simulation, transient simulation platforms, and heat transfer effects on transient performance. An overview is illustrated in Fig. 1. In Section 2, the development and application of the transient performance simulation methodology will be discussed. In Section 3, the development and comparison between gas turbine transient simulation platforms will be discussed. In Section 4, the heat transfer effects simulation methodologies for the heat soakage effect, tip clearance effect and component characteristic change effect will be discussed. In Section 5, the current status, challenges, and future for gas turbine transient simulation will be discussed. Finally, Section 6 will offer a conclusion of the transient performance analysis progress.

2. Gas turbine transient performance simulation

The change in engine performance as a result of altering the fuel flow is referred to as transient operation. This process can last anywhere from a few seconds in the case of aero engines to several hours for large industrial gas turbines [2]. Since civil aero engines need to meet the certification requirement and the starting time of a large industry turbine is a critical economic indicator, the transient performance plays a crucial role in gas turbine analysis.

Over the past 70 years, extensive research has been conducted on the development and improvement of gas turbine transient performance prediction. Many comprehensive surveys of this research have been published, including those by Fawke and Saravanamuttoo, Szuch, Evans and Sanghi [4–7]. These surveys provide a broad overview of the development of transient simulation from 1950 to 2000. Based on the comprehensive review, the gas turbine overall transient methodology can be broadly classified into two categories: the white box and the black box approach [9]. The fundamental ideas of these two approaches are different. The white box approach involves using physics-based models, where the dynamic equations, thermodynamic relationships, and energy balance are considered. On the other hand, the black box approach involves the use of the ANN, machine learning, or deep learning techniques when direct access to the complex dynamic equations of the system is not feasible or when working with them is challenging [11]. Moreover, numerical approaches have also been applied in the gas turbine overall transient simulation. It offers a detailed insight into the

flow field that cannot be provided by the white box and black box approaches. In this section, the development of the white box, black box and numerical methodologies will be discussed.

2.1. White box approach

White box models usually represent the physics-based models or mathematical models that deal with coupled and complicated dynamic equations, thermodynamic relationships, energy balance, and linearization methods [11]. According to the published resources, the white box method can be broken down into linear and non-linear methods. In this section, they will be discussed in chronological order, tracing the progression of its methodology development, as well as related transient investigation work.

2.1.1. Linear method

The analysis and experimental study of the dynamic characteristics of gas turbines began in the early 1950s [12] and aimed at meeting engine control needs. Researchers from National Advisory Committee for Aeronautics, Otto and Taylor, were the first to investigate the rotor speed response of a single-spool turbojet engine with a step change in fuel flow using a first-order system [13]. The equation used to describe the first-order lag system is shown in Eqs. (1):

$$(I^* \sqrt{\theta^*} d(\Delta N)) / (\delta^* b^* dt) + \Delta N = (a/b)^* \Delta (W_f \eta_b) \quad (1)$$

where I is the polar moment of inertia of rotating parts, θ is the altitude temperature ratio, ΔN is the difference between transient shaft rotational speed and steady-state shaft rotational speed, δ is the altitude pressure ratio, b is partial of torque with respect to engine speed at constant values of either actual or effective fuel flow, a is partial of torque with respect to either effective or actual fuel flow at constant engine speed, W_f is the fuel flow, and η_b is the combustion efficiency. Because the accelerating torque can be represented as a function of fuel flow and spool rotational speed, they used a linear differential equation obtained from the steady state to represent the acceleration behaviour with a speed change range of less than 600 rpm.

Then it was realized that the engine dynamic performance could be predicted from the steady state data, and the calculation of the rotor-

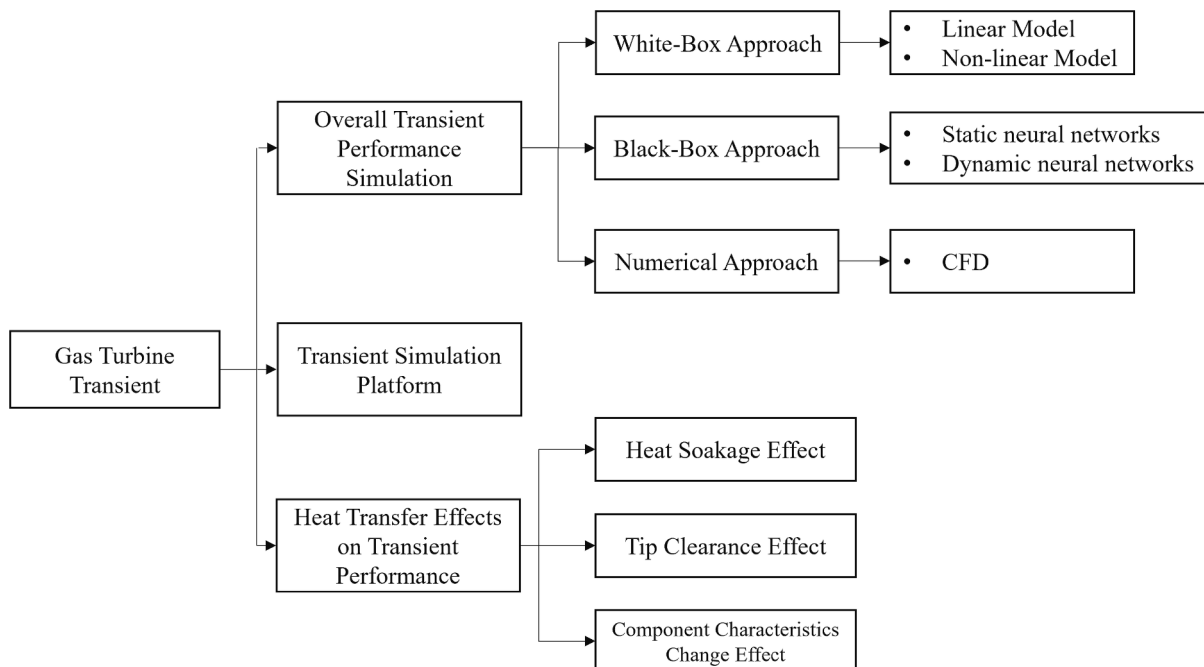


Fig. 1. Overview of gas turbine transient simulation and heat soakage effect approaches.

speed time constant became the focal point of the research. Gold and Rosenzweig developed a method for estimating the rotor-speed time constant for both turbojet and turbine-propeller engines [14]. For turbojet engines, the method required the variation of steady-state air flow and steady-state compressor temperature rise with engine speed and the polar moment of inertia of an engine. For turbine-propeller engines, additional propeller torque data was needed. The results showed that the calculated values deviated from the mean experimental values by only slightly more than the spread of the experimental data. Similarly, Lawrence and Powell developed a good approximate method that assumed the turbine torque changes when fuel flow changes but zero change in compressor torque [15]. With this assumption, the time constant of a single-spool gas turbine can be expressed as Eq. (2):

$$\tau = k^* I^* N^* \left(\frac{dW_f}{dN} \frac{\Delta T}{T} \right)^{-1} \quad (2)$$

where k is a dimensionless constant, N is the shaft rotational speed, ΔT is the temperature drop across the turbine, T is the turbine inlet temperature. All parameters used in the time constant could be readily obtained from steady-state data, making it easy and convenient to establish the time constant.

The next major contribution was made by Novik, who extended the current linear single-spool turbojet engine into a two-spool engine by applying a second-order linear system [16]. The relation between spool speed and turbine inlet temperature was estimated experimentally, and the method was able to specify different spool speed responses.

The linear system is capable of representing the gas turbine transient performance. However, it could only simulate engine transient operating points with minor changes [13]. Therefore, it was impossible to obtain the compressor's operating trajectories. The development and implementation of a non-linear system were necessary to obtain more accurate results.

2.1.2. Non-linear method

The non-linear approach was initially introduced by Dugan and Fillipi [17,18]. Their research focused on investigating the acceleration performance of a twin-spool turbojet engine, by determining a set of operating points that satisfied flow compatibility.

The constant Mass Flow (CMF) method, also known as the iterative method, was developed by Larroche et al. using an analogue computer [19]. This method assumed that flow compatibility was always maintained, even during the transient condition. The simulation process was carried out in three steps. Firstly, the initial engine component outlet pressure and shaft rotational speed were obtained based on the starting condition of the transient process. Next, the engine parameters, such as the compressor pressure ratios and turbine non-dimensional flows, were estimated and iterated while keeping the rotational speed constant and ensuring that flow compatibility was satisfied after a step change in fuel flow. Finally, with the new component working condition, the compressor power (CP) and turbine power (TP) could be calculated, and the rotor angular acceleration could be determined based on the surplus power (SP). The new rotational speed after a one-time step could then be obtained. The governing equations used in this process are listed in Eqs. (3)–(5),

$$SP = TP - CP \quad (3)$$

$$dN/dt = SP/(4\pi^2 I^* PCN_{old} * N_{DP}) \quad (4)$$

$$PCN_{new} = (PCN_{old} * N_{DP} + (dN/dt) * \Delta t)/N_{DP} \quad (5)$$

where dN/dt is the rotational change rate, PCN_{old} is the corrected rotational speed at the last time interval, N_{DP} is the design point rotational speed, PCN_{new} is the corrected rotational speed at this time interval, and Δt is the time interval. The complete engine computer assembly was composed of engine components assemblies. Due to the equations

concluded in each component assembly, the flow compatibility was satisfied automatically. Fig. 2 shows the process of CMF calculation, where 1–4 subscripts mean compressor inlet, compressor outlet, combustor outlet and turbine outlet.

Several gas turbine studies have been investigated based on the utilization of the CMF method. Kong et al. analyzed the steady state and transient performance of a 200 kW class small turboshaft engine with a free power turbine [20]. It was found that the turbine inlet temperature exceeded the limit temperature by 0.3 s with the step change in fuel flow. Compared with experimental data, the maximum range of error was within 5.56%. The transient performance of a geared turbofan engine was investigated by Wanjun and Shijian by using the CMF method [21]. The outcome was compared with the result calculated from GasTurb 10, and the maximum difference was within 1.5%. However, they didn't fully explain the benefit coming from the application of gearbox in their paper. The transient performance of hybrid propulsion systems was investigated by Wortmann et al. [22]. Two types of gas turbine engines had been examined with the design parameters from GasTurb 12. The outcome showed that the acceleration time of the hybrid gas turbine can be reduced by 50% when the motor shares 25% of the shaft power. The transient performance of the T100 micro gas turbine (mGT) in the wet mode for critical surge conditions was investigated by Carrero et al. [23]. This study simulated the engine performance under certain conditions and assessed the potential effect on power output. It was found that the wet mode will decrease the surge margin during the transient process, and the acceleration and deceleration speed should be limited. Further investigation on the effect of fuel composition change on T100 mGT transient performance was done by Raggio et al. [24]. It was found that sudden injection of hydrogen led to an excessive temperature peak, while in the case of ammonia, high temperatures were not reached. An in-house program, especially for the mGT transient simulation, was developed by Kim et al. [25]. The CMF method was used during the transient simulation. Besides, a quasi-2D recuperator model was established to offer a realistic counter-flow compact heat exchanger.

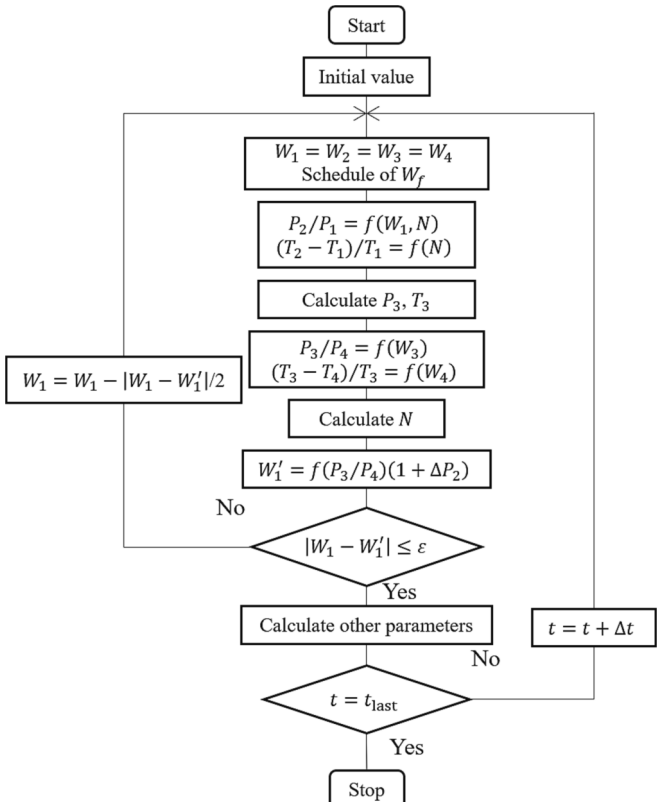


Fig. 2. Flow chart of the CMF method.

The transient performance of a solid oxide fuel cell and mGT hybrid system has been investigated by Mueller et al. by CMF method [26]. It was showed that SOFC/mGT hybrid systems could have a rapid transient load following capability that is faster than that of recuperated mGTs. Singh et al. [27] investigated the transient behaviour of an industrial gas

turbine operating on low-calorific fuels based on the CMF method. Engine transient behaviour during a load shed and engine trip with varying fuel LHV was investigated. It was found that lower LHV fuels tend to result in higher rotor over-speeds in case of a load shed and require a shorter valve closing time.

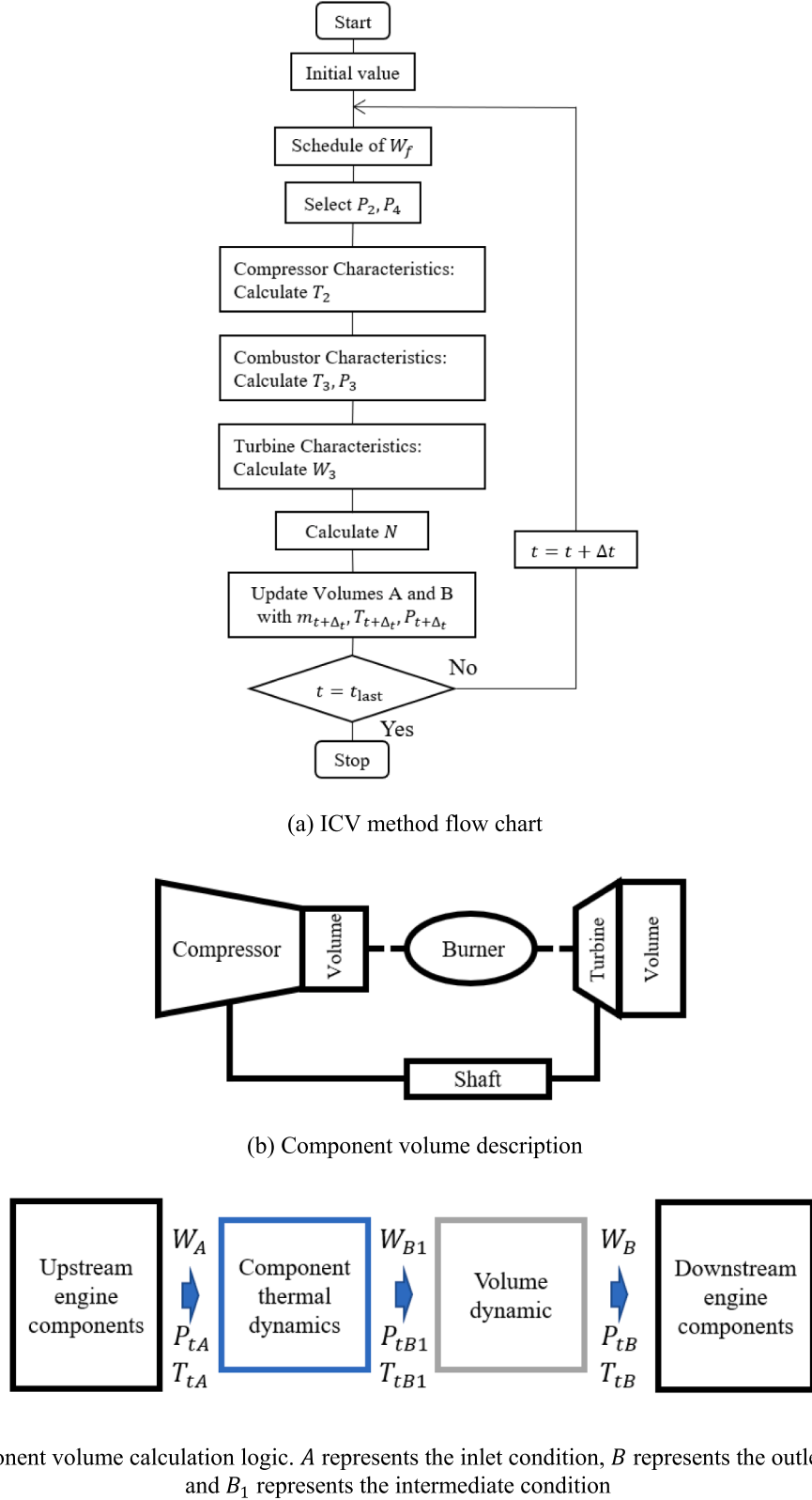


Fig. 3. ICV method illustration.

The next major advancement in gas turbine simulation was the Inter-Component Volume (ICV) method developed by Saravanamuttoo and Fawke, which considered the volume dynamics in its calculation [28]. Fig. 3 (a) shows the process of ICV calculation. In this method, the flow was treated as discontinuous. The gas turbine model was composed of a series of discrete components, each consisting of two parts: an actuator disk and a lumped volume, as shown in Fig. 3 (b). The calculation process is shown in Fig. 3 (c). The component thermal dynamic block was used for component performance calculation without considering volume dynamics, resulting in the same mass flow at positions A and B1 ($W_{B1} = W_A$). The volume dynamics block only considered the effect of volume, leading to a difference in the mass flow at positions B1 and B ($W_B \neq W_{B1}$). At each time interval, the component flow mismatch was used to calculate the change rate of component inlet/outlet parameters, as listed in Eqs. (6)–(9),

$$m_t = P_{st}/(R*T_{st})*Vol \quad (6)$$

$$m_{t+\Delta t} = m_t + (W_{in} - W_{out})*\Delta t \quad (7)$$

$$T_{st+\Delta t} = \frac{(W*Cp*\Delta t*T_{st})_{in} + (m_t - W_{out}*\Delta t)*Cp*T_{st}}{(W*Cp*\Delta t)_{in} + m_t*Cp - W_{out}*\Delta t*Cp} \quad (8)$$

$$P_{st+\Delta t} = (R*T_{st+\Delta t} * m_{t+\Delta t})/Vol \quad (9)$$

where m_t is the mass stored in component volume at time t , P_{st} is the static pressure at time t , R is the gas constant, T_{st} is the static temperature at time t , Vol is the component volume, W is the mass flow rate, Cp is the specific heat. The new mass flow was then used for component work calculation and rotor acceleration rate calculation.

The volume packing effect had been extended from the main component volume to additional secondary air systems that include rotating pump components (such as rotating cavities between compressor or turbine disks), pressure loss components (such as pipes, labyrinth finned seals, orifices), and volume packing components (such as ducts and cavities) by Chuankai et al. [29]. Similar to the ICV method, the method modified the component outlet mass flow and the enthalpy based on the change in volume parameters. The continuous equation and energy equation are listed in Eqs. (10)–(11). After the simulation on a turbofan engine during the acceleration and deceleration process, it is found that the disk cavities will significantly reduce the coolant flow for the turbines and might lead to potential adverse transient thermal load on the engine.

$$W_{out} = W_{in} - \frac{Vol}{\gamma*R*T_s} * \frac{dP_s}{dt} \quad (10)$$

$$h_{out} = \left[W_{in}*h_{in} - (W_{in} - W_{out})*u - \frac{P_s * Vol}{R*T_s} \frac{du}{dt} \right] / W_{out} \quad (11)$$

where γ is the ratio of specific heats, h is the enthalpy, and u is internal energy.

Several studies have examined the choice of the ICV method. Chung et al. developed a dynamic model based on governing equations to investigate the compressor stall effect on aero-engine transient performance and the effectiveness of stall recovery control strategies [30]. The model consisted of various components represented by 1-D and 2-D control volumes. According to the authors, the developed model was capable of simulating in-stall transients induced by inlet temperature ramping, main burner fuel pulse, and inflow bleed. However, the authors also noted that the heat transfer effect, transonic effect, and start stall effect should be included in further analysis. The immediate effects of water ingestion on the transient performance were investigated by Haykin and Murthy by establishing a generic, high bypass ratio engine model that was based on the ICV method [31]. The mass fraction of the water varied from 0% to 8%, and effects on the air compression system and burner were considered. A non-linear relation between the change

in compression subsystem performance and the amount of water is found, and this change in compression subsystem performance will have an unmanageable effect on engine transient performance, especially during engine deceleration when water mass fraction is high. The steady-state and transient performance of a twin-spool mixed-flow turbofan engine was investigated by Yadav et al. [32]. The method used was a modified version of the ICV method. Different from the other researchers who validated their data with experimental data, the validation was against the result from the Gas turbine Simulation Program (GSP). The transient performance of externally fired mGTs was investigated by Traverso et al. based on the TRANSEO platform [33,34]. The ICV method was implemented with the consideration of interconnecting volume between two consequent components. The simulation outcome was compared with experimental data and showed good accuracy. Wang et al. investigated the gas turbine fuel system based on the ICV method [35]. The simulation outcome showed that the fuel system would delay the transient performance for 0.5 s. Shamekhi et al. investigated the transient performance of a concentrated solar power mGT during the start-up phase based on the ICV method [36]. Validation was provided for both sub-element (solar receiver and recuperator) performance and overall transient performance, and a good agreement with errors less than 0.6% was achieved.

CMF and ICV methods have their advantages and disadvantages and will lead to a different component transient working line. Saravanamuttoo and Fawke noted a significant difference between these two methods on the compressor working line when there was a rapid change in fuel flow. In Fig. 4, an instantaneous move from 0 to 0' then up the line 0'1 (line A) can be found when using the iterative method. However, the working line by using the ICV method would follow line B [37]. It was also mentioned that the CMF method required more calculation time per point due to the iterative process but could take a larger time step, while the ICV method required less calculation time per point, but a smaller time step was necessary. The CMF method was suitable for long-term transient simulation due to its larger time step tolerance, while the ICV method was more suitable for short-term transient simulation. Nishi and Sawada mentioned that when the complexity of the engine increases, the convergence in the CMF method would become more difficult to meet and would lead to a longer

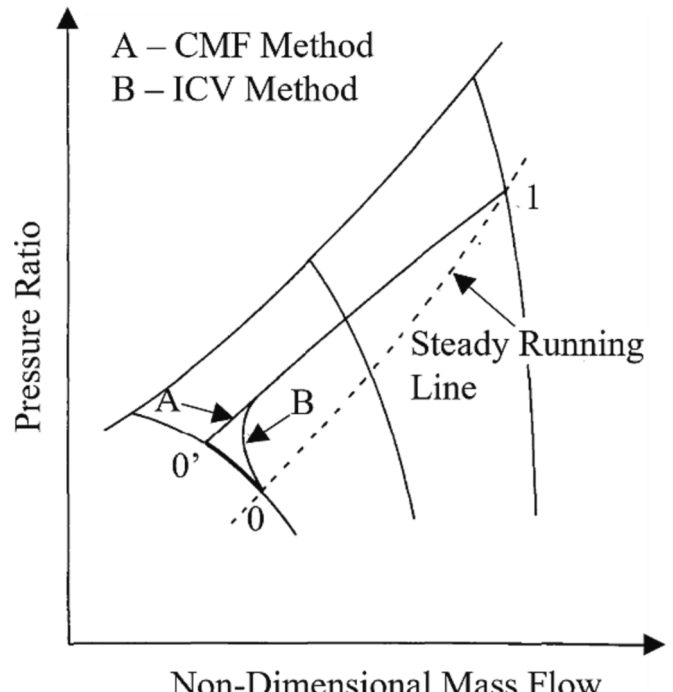


Fig. 4. The comparison of operating trajectories for CMF and ICV method [4].

calculation time [38]. Pilidis also highlighted the strengths and weaknesses of each method [39]. He mentioned that convergence in the ICV method was occasionally difficult and depended on the choice of time step length. With an unsuitable time-step length, the convergence time of the model was longer and may even slightly oscillate [21]. Naylor pointed out that the ICV method was more suitable for fast transient simulation, while the CMF method was more suitable for slow transient simulation, where the assumption of zero mass flow accumulation within components was more justifiable [40]. Additionally, Rahman and Whidborne reported that the CMF method was slightly more accurate than the ICV method [41]. However, the calculation speed and suitability for complex gas turbine models made the ICV method more appropriate for real-time transient simulation [21].

The ICV method, while considering volume dynamics, assumed that pressure propagates immediately throughout the volume, which could lead to inaccuracies when the volume is large. To address this issue, the Pressure Wave in Volume (PWV) method was developed by Li et al in 2001 [42]. The PWV method considered four types of pressure waves (PW): PW from the turbine, PW reflection from the nozzle, PW reflection from the turbine, and PW passing through one another. The calculation process of velocity V , which was used to modify temperature and pressure, is shown in Eqs. (12),

$$V = V_0 + \frac{2^*a_0}{\gamma - 1} \left[(P_s/P_{s0})^{(\gamma-1)/2\gamma} - 1 \right] \quad (12)$$

where V is the velocity, a is the speed of sound and subscript 0 means undisturbed gas in front of the wave. A comparison between the PWV and ICV methods was illustrated based on the simulation outcome of a two-spool turbojet engine. The author stated that the PWV method reflected better gas turbine transient performance. Although the difference between the two methods was small, it could be bigger when considering large volumes such as a bypass duct. However, due to a lack of testing programs and data, the accuracy of the predicted pressure wave effect on the gas turbine transient performance is difficult to validate. The calculation time was also significantly increased, taking 8 min compared to 5 s for the ICV method.

A hybrid approach that combined ICV and CMF methods was developed by Rahman and Whidborne [41] to alleviate the weaknesses of CMF and ICV methods (slow calculation speed for the former and lower accuracy for the latter). The idea was to use the ICV method to calculate the mass flow accumulation inside the component volume and then utilize the CMF method to solve the thermodynamic algebraic equations associated with each component. A three-spool turbofan engine was selected, and a deceleration transient process was simulated in the hybrid and CMF methods. Results showed that the hybrid approach provided results close to those of the CMF method but with significantly faster calculation speed. However, the turbine map used by the CMF method was based on the enthalpy work function, while the hybrid method was based on the pressure ratio. This difference in the turbine map resulted in offsets in compressor working lines, especially for the high-pressure compressor (HPC) working line. Nevertheless, the hybrid approach had the potential to improve accuracy compared to the ICV method [43].

Apart from the PW problem mentioned above, the ICV method was prone to slow convergence because it required interaction with the components' map. This was observed under certain conditions, such as when the compressor speed line was nearly horizontal and one pressure ratio corresponded to different mass flow values. To address this issue, Li proposed the imbalanced mass flow (IMF) method in 2019 [44]. The IMF term was calculated using volume dynamics and was added to the corresponding component to rebalance mass flow during the iteration process, which is illustrated by Eqs. (13)–(14). This method combined the advantages of the traditional ICV and CMF methods, presenting the effect of mass storage and having no limitations on map reading due to its iterative matching procedure. However, when comparing the

outcome with the CMF and ICV methods, a maximum difference of 9.8% was found, higher than other researchers' outcomes. Also, the author didn't mention the time step and calculation speed of the methodology.

$$IMF = \frac{dm}{dt} = \frac{dP_*}{dt} \frac{Vol}{R*T_t} \quad (13)$$

$$IMF = W_{in} - W_{out} \quad (14)$$

2.2. Black box approach

The black box approach, also known as a data-driven based model, differs from the white box approach in that it relies on operational data from system performance measurements or data generated through physics-based models. Instead of focusing on dynamic equations, thermodynamic relationships, and energy balances, the black box approach focuses on the relationship between input and output data. One of the most significant methods in the black box approach is the use of ANN. ANNs are computing systems comprised of simple, highly interconnected processing elements (neurons) with linear or non-linear transfer functions. These elements process information by dynamically responding to external inputs [45]. The use of the ANN models in gas turbine transient simulation emerged much later than the white box approach, and a limited number of studies focused on transient analysis because most of the ANN models were mainly used for static performance analysis [46]. However, despite limited research, the black box approach is still worth discussing as it may be one of the main development directions. Chiras et al. reviewed the initial development of black box methodologies [47]. While Asgari and Chen's book on ANN application for gas turbine modelling simulation and control also includes a brief review of black box approach development [45]. There are different types of ANN, including (but not limited to) multi-layer perceptron (MLP), radial basis function neural networks (RBF), convolutional neural networks (CNN), modular neural networks, and recurrent neural networks (RNN). These ANN models can be split into two categories: static (feedforward) neural networks (including MLP, RBF) and dynamic (feedback) neural networks (including RNN). This section will cover static networks, dynamic networks, and other black box approaches. However, only directly linked ANN based gas turbine transient performance models will be described in detail.

2.2.1. Static network (Feedforward)

Static neural networks are the simplest neural networks and are characterized by memory-free non-linear equations, which means that there is no feedback element and no delay in the network. Therefore, the output parameters of the static neural network only depend on the current values of the input parameters.

The MLP neural network (NN) is the best-known type of static network model [45]. The MLP NN is composed of an input layer, one or more hidden layers, and an output layer. Dot products are applied between inputs and weights. And sigmoidal activation functions are normally applied to the hidden layer. A simple structure of an MLP NN model is illustrated in Fig. 5, where the blue dots represent the input layer, the orange dots symbolize the hidden layer where the estimation takes place, and the green dots depict the output layer. The output of the MLP NN can be described by Eq. (15).

$$y = f \left(\sum_{i=1}^n w_i * x_i + b \right) \quad (15)$$

where y is the output of the NN, f is the function, w_i is the i th connection weight, x_i is the i th input of the NN, and b is the hidden layer. All connection weights and the hidden layer will be trained during the learning process to minimize the forecasting error of the NN.

This kind of model was simple and easy to train and had been used by Ruano et al. to analyze the shaft speed dynamic of the Rolls-Royce Spey

Input Layer

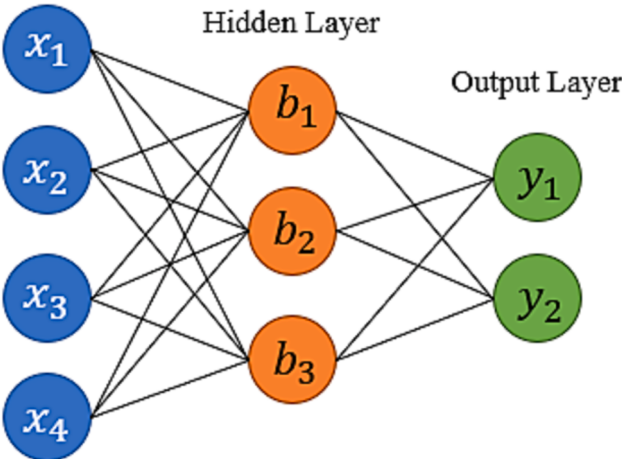


Fig. 5. A simple structure of an MLP NN with input, hidden, and output layers.

engine [48]. Two topologies of MLP NNs, with one and two hidden layers, were experimented with. It was concluded that MLP NN can provide a promising outcome, and MLP NN with two hidden layers can provide a more accurate outcome. Gambarotta et al. used MLP NNs to simulate the transient performance of mGT [49]. Instead of applying the black box approach to the whole system, only the compressor and turbine were considered. It was reported that using MLP NNs could reduce the calculation time and make the simulation suitable for real-time simulation. A lack of a methodology that can generate a good set of training data for the whole operating range and the flight envelope was mentioned by Rezvani et al. [50]. To fulfil this area, the MLP NN was used with the combination of the design of experiments methodology. The input data for the NN were altitude, Mach number, ambient temperature and fuel flow profile, and the net thrust, turbine entry temperature, and compressor corrected mass flow were the outputs of the NN. The simulation outcomes had been compared with the physically based model, and the differences in outputs were controlled within 2%. Rahnama et al. also used the MLP NN model to predict the performance of the GE 9001EA heavy-duty gas turbine [51]. Air temperature, shaft rotational speed, fuel stroke reference and inlet guide vane position were the input of the MLP NN and were used to predict the electrical output power and exhaust temperature of the gas turbine. The mean squared error for output power and exhaust temperature is 0.355 and 17.708, separately. It was mentioned that the MLP NN has the potential to offer a more accurate outcome than conventional non-linear models. Khalili and Karrari compared the MLP NN based gas turbine model with the white box based model and the outcome showed that the MLP NN based model could offer better accuracy on predicted power output and exhaust gas temperature [52]. Koleini et al. investigated the effect of hidden layer number on MLP NN prediction accuracy for gas turbine exhaust gas temperature prediction during transient [53]. It was concluded that the model with more hidden layers had a better capability.

Another feedforward network is the RBF NN. Like the MLP NN, RBF NN also has the input, hidden, and output layers. A simple structure of an RBF NN model is illustrated in Fig. 6. However, between the input and hidden layers, a non-linear transformation containing radial basis activation functions is utilized. Besides, a Gaussian function is used in the hidden layer as the transfer function in computational units. The output of the RBF NN can be described by Eqs. (16)

$$y = \sum_{i=1}^n w_i * \varphi(\|x - x_i\|) \quad (16)$$

Input Layer

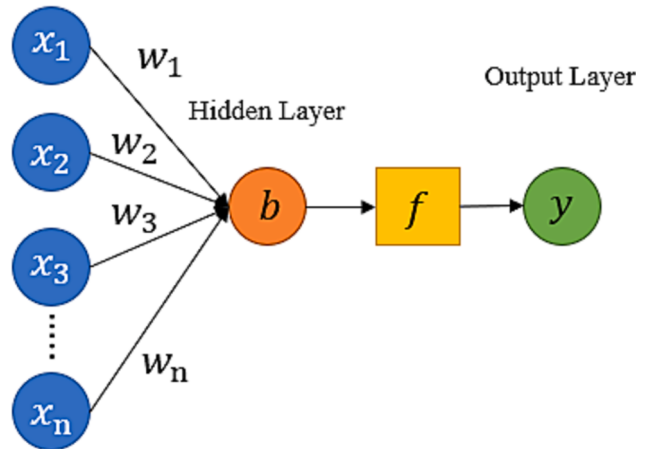


Fig. 6. A simple structure of an RBF NN with input, hidden, radial basis function and output layers.

where φ is a real-valued function to represent the distance from an origin, and x is the origin. Compared with MLP NN, RBF NN needs a smaller number of hidden layers (one hidden layer is quite enough). Networks of this type can speed up and simplify data processing. Depending on the case, it is typically observed that the RBF NN requires less time to reach the end of training than MLP NN. However, RBF NN needs more training requirements due to the radial basis functions between the hidden layer and output layer.

Kim et al. utilized an RBF NN to calculate the performance of a gas turbine for aircraft engines during transient operations [54]. The input parameters used for training the RBF NN were the altitude, flight Mach number, fuel mass flow rate and additional power due to the moments of inertia of the rotating parts. The output parameters in the data-driven model were engine net thrust, shaft rotating speeds, the pressure and temperature at each station and efficiencies. Two types of RBF NNs were investigated. One was the conventional structure with no iterative process. The other was a proposed model with an iterative calculation. It is mentioned by the author that the latter RBF NN that includes an iterative calculation can offer a better similarity with the first principal model based on NPSS. Wu also applied an RBF NN to estimate the transient performance of a split-shaft gas turbine [55]. The model was first used for predicting the characteristic curve of the compressor and then for the transient performance prediction. It was mentioned by the author that the RBF model had higher training speed and better time control performance and it was suitable for dynamic simulation which has a higher time requirement.

2.2.2. Dynamic network (Feedback)

A dynamic neural network is a type of neural network that can change its structure or topology during runtime based on the input data it receives. In other words, the network can adjust its architecture to best fit the input it is currently processing. This is in contrast to a static neural network, which has a fixed structure and cannot change its architecture during runtime. A comparison between the static neural network and the dynamic neural network has been investigated by Ibrahim et al. [56]. There are several types of dynamic neural networks, such as RNN, which have a “memory” that allows them to process sequences of variable length, and transformers, which use a self-attention mechanism to weigh the importance of different parts of the input sequence. Based on the comprehensive review, non-linear autoregressive exogenous (NARX) models, which is a type of RNN, are commonly used by researchers [57]. In this section, research related to the application of the NARX model on gas turbine transient simulation will be focused on.

NARX is a non-linear autoregressive network with exogenous inputs

[58]. It has a recurrent dynamic nature and is commonly used in time-series modelling. The NARX model is defined by Eq. (17):

$$y(t) = f[x(t-1), x(t-2), \dots, x(t-n_x), y(t-1), y(t-2), \dots, y(t-n_y)] \quad (17)$$

$$RMSE = \sqrt{\frac{1}{n_d} \sum_{i=1}^{n_d} \left(\frac{y - y_m}{y} \right)^2} \quad (18)$$

where $y(t)$ is the output of the NARX model, f is a non-linear function based on $y(t)$ and $x(t)$, $x(t)$ is the input of the NARX model, and n_x and n_y are the number of past output and input terms. During the training process, the root mean square relative error (RMSE) is commonly used to determine the goodness of the training outcome. The definition of RMSE is shown in Eqs. (18), where n_d is the number of datasets, y is the available (simulated) data, and y_m is the prediction of the NARX model. The structure of a typical NARX network is shown in Fig. 7. The blue dots represent the input layer, the purple dots represent the recurrence layer, the orange rectangle symbolizes the NARX hidden layer where the estimation takes place, and the green dots depict the output layer.

NARX models had been used to estimate gas turbine transient performance in many studies. The transient performance of mGT in non-isolated mode was investigated by Jurado based on the NARX model [59]. Intentionally tripping one generator was simulated, and it was found that the whole system needed 5 s to return stability. Asgari et al. developed a NARX model to simulate the start-up simulation of a heavy-duty gas turbine [58,60]. The simulation outcome compared with the experimental data is illustrated in Fig. 8. The model consisted of three input variables and four output variables. The inputs were compressor inlet temperature, compressor inlet stagnation pressure, and fuel flow rate. The outputs were compressor outlet temperature, turbine outlet temperature, compressor pressure ratio, and rotational speed. After training, the RMSE for the four outputs was limited to 12%. To verify the models, they were tested against three other available experimental data sets. The results showed that the NARX models can effectively capture and predict GT dynamics during the start-up process. The deviations between measured and simulated values were generally acceptable, with compressor and turbine outlet temperatures having a maximum deviation of approximately 3.5%. However, deviations could be higher for compressor pressure ratio and rotational speed, with maximum deviations of 7.4% and 7.1%, respectively. A further comparison between the open-loop NARX model and the close-loop NARX model was

investigated by Asgari et al in 2021 [61]. It was concluded that the open-loop NARX model had a better performance with higher accuracy compared to the closed-loop NARX model. Yu et al. [62] employed fuel-air-ratio and ambient conditions, including flight altitude and Mach number, as input values of a NARX model to simulate the transient performance of a turbofan engine. Among the four established NARX models, the best one could have a fitting degree of 96.43% on LP shaft rotational speed and 96.95% on HP shaft rotational speed. Bahlawan et al developed a NARX model for a heavy-duty single-shaft gas turbine to investigate the cold, warm and hot start-up transient performance [63]. 14 measured time series (6 for cold start-up, 6 for warm start-up, 2 for hot start-up) were selected to train the NARX model. However, the author did not give detailed information on the input data series. The RMSE values for the estimated compressor outlet temperature, turbine outlet temperature and rotational speed were controlled within 2% when the value is within 2.5% for the compressor pressure ratio. To address the single neural model's limitations (low accuracy when the model operates outside the field in which it was trained and long training time), an ensemble of multiple-input single-output NARX models had been developed by Ibrahim et al. [57]. This model used different configurations to represent each output parameter with the same input parameters. According to the author, the novel model could represent the transient performance of a three-spool aero-derivative gas turbine engine during the full operating range with good accuracy, even with different input scenarios from different operation conditions.

Except for the NARX models, the ability of deep learning and machine learning techniques to predict gas turbine transient performance had been investigated by researchers. A machine learning-based model of a single-shaft gas turbine was developed by Asgari and Ory in 2021 [64]. RNN was employed to train the datasets of the GT variables. The results demonstrated that the RNN models were capable of performance prediction of the system with high reliability and accuracy. A deep learning convolutional neural network was developed by Alsarayreh et al to predict the transient performance of a dual-fuel gas turbine [65]. The inputs for the model were the natural gas, control valve, pilot gas control valve and compressor variables, whereas the outputs for the model are output power, the exhaust temperature and the turbine speed or system frequency. However, the comparison with a NARX model showed a slight inferiority in the accuracy of the deep learning model.

2.3. Numerical approaches

Except for the white box and black box approaches, the computational fluid dynamics (CFD) method also plays an essential role in the aerodynamic design of turbomachinery. It can shorten the design cycles to better performance and reduce design costs.

CFD simulations involve several key steps: geometry creation, mesh generation, boundary condition setting up, physics modelling, and numerical solving. During the geometry creation, the geometry of the targeted turbomachinery is created or imported to capture the features of the flow field, including solid objects, boundaries, and fluid regions. During mesh generation, a computational mesh is generated over the geometry, dividing the domain into discrete cells or elements. The mesh captures the spatial resolution and discretizes the equations for numerical solutions. The boundary condition of the flow field was then set up. During the physics modelling, various physical phenomena such as turbulence, heat transfer, and multiphase flow are considered. Different turbulence models can be employed. In the last step, the Navier-Stokes equations and any additional models and boundary conditions are solved using numerical techniques, such as finite volume or finite element methods.

Nowadays, modern compressor and turbine design would face great difficulty without the help of CFD. CFD method can be divided into two categories. One is the steady-state CFD method, and the other is the transient CFD method. The steady-state CFD method refers to the use of methods like Reynolds averaged Navier Stokes. In this type of CFD

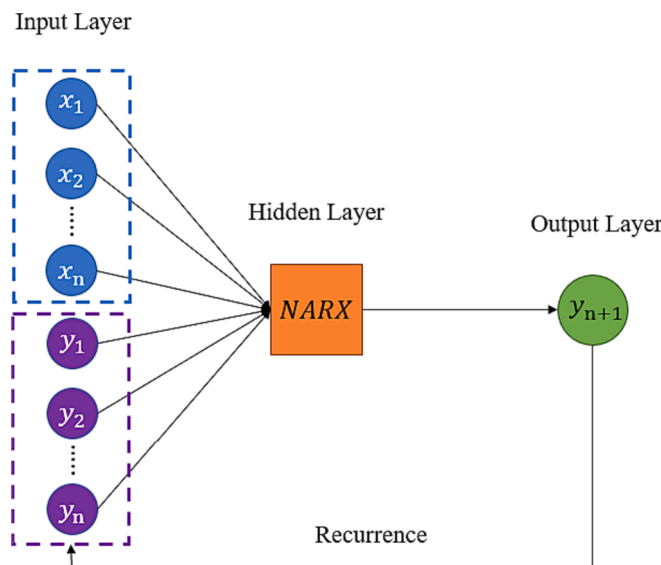


Fig. 7. A schematic of a typical NARX network.

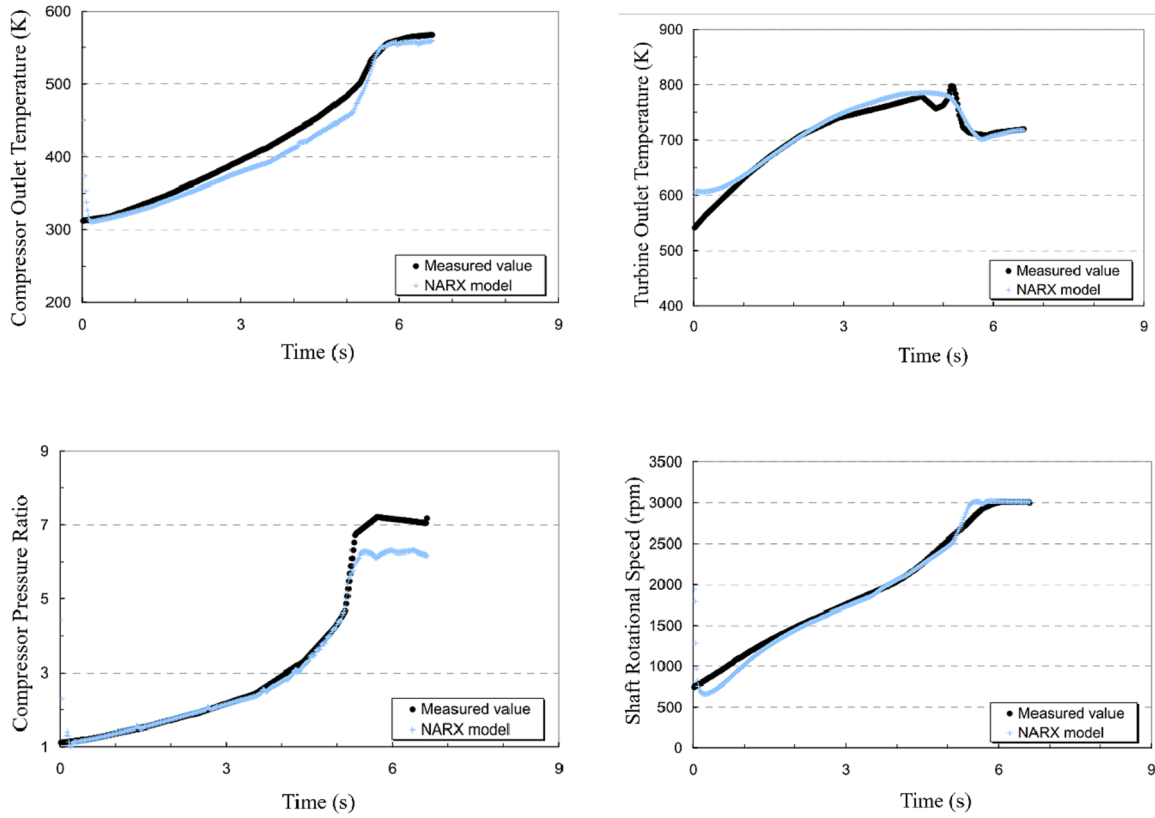


Fig. 8. Gas turbine transient performance comparison between the NARX model and experimental data [46].

method, time-averaged outcomes will be calculated. The transient CFD method refers to the use of methods like large eddy simulation (LES) and direct numerical simulation. Different from the steady state CFD method, transient CFD methods provide time-dependent information and are suitable for studying unsteady flow phenomena, such as vortex shedding, flow instabilities, and turbulent mixing. Since this review paper aims to illustrate the full picture of the gas turbine transient simulation, only the transient CFD method will be included. Moreover, this section is concerned with the application of CFD and does not describe the numerical methods or turbulence modelling in any detail.

Since CFD predictions became central in the design process of turbomachines, many investigations had been launched in this area [66]. Denton and Dawes reviewed the development of the CFD method for turbomachinery design from the 1940s to 1990s [67]. However, due to the limitation of CFD method development, only a very limited transient CFD method was introduced. Tyacke et al. offer a more recent review on this topic up to the 2020s [68]. The LES method was focused on.

Based on the review, it was found that CFD was mainly applied at the component level in the gas turbine transient performance field. Blumenthal et al. investigated the transient performance of NASA Rotor 35/Stator 37 stage transonic compressor stage by using both steady and transient CFD methods [69]. The simulation outcome was compared with experimental data, and it was reported that the transient CFD method could offer a slightly better outcome. Qizar et al. also investigated the transient performance of NASA Rotor 35/Stator 37 stage [70]. The aerodynamic performance of a high-pressure turbine was investigated by Murari et al. by five types of CFD methods, including mixing plane approach, frozen rotor approach, scale adaptive simulation, detached eddy simulation, and LES [66]. The outcome showed the advantages of LES in vortex shedding prediction. Roclawski et al. investigated the transient performance of a radial turbine during load step operation conditions [71]. The turbine CFD model was integrated into the transient loop, where the CFD model would directly estimate the

turbine power instead of using conservation equations. Instead of the dynamic performance of the component, CFD is also capable of generating the component off-design characteristic map, which can be used during the gas turbine overall transient performance simulation. Cornelius et al. investigated the off-design performance of a multistage axial compressor [72]. Both steady and transient CFD methods were used. The performance of a multistage compressor equipped with a variable inlet guide vane was investigated by Kim et al. by using both steady and transient CFD methods [73]. The generated component map could offer a good agreement when comparing with the experiment data. Mohammadian et al. investigated the startup transient performance of an industrial gas turbine with the aid of CFD [74]. The component characteristic maps were generated by CFD based on the real component geometry instead of using a general map.

However, it was found that CFD is not used extensively for predicting the gas turbine overall transient performance due to the extremely high computational cost [75,76]. Marsilio developed a CFD-based turbojet engine transient performance model [77], where the engine was divided into five modules: inlet, compressor, combustor/turbine and nozzle. The modular architecture separated the engine and made it easier to run simulations. The fluid dynamic field in each module was determined numerically using a CFD 1D method and the boundary conditions were based on the engine operating points. The governing equation is the time-dependent Euler equations written in their integral form as in Eq. (19):

$$\frac{\partial}{\partial t} \int_v \vec{W} dv + \int_S \vec{F}_t \cdot \vec{n} dS = 0 \quad (19)$$

where v is an arbitrary volume enclosed in a surface S , \vec{W} is the hyper-vector of conservative variables and \vec{F}_t is a combination of inviscid fluxes. Ferlauto improved Marsilio's work to a high bypass turbofan engine [78,79]. Compared with the engine model developed by Marsilio, the module number was increased from 5 to 10. The flow field

around the engine was simulated by a standard CFD technique (2-D grid), as shown in Fig. 9 (a), while the engine core was represented by the 1D CFD model based on Marsilio's method, Fig. 9 (b). That was required to alleviate the extremely high computational cost and required geometry data for a full 2D engine simulation. Each compressor and turbine blading was simplified as a discontinuity surface with its left and right boundaries based on the actuator disc theory [80]. The boundary conditions of the inlet and outlet area depended on engine's operating conditions. For the subsonic inlets and outlets, total and static pressure, total temperature and the flow angle were needed. For the supersonic inlets and outlets, all the flow variables were necessary. An acceleration process from idle to maximum throttle was simulated. The simulation outcome of the Mach number contours of the external flow during engine transient is shown in Fig. 10.

In conclusion, the numerical method (CFD) has the potential in predicting the gas turbine transient performance. However, due to the extremely high computational cost on 2D or 3D CFD models and the need of detailed geometry data, this method has not been widely applied in gas turbine transient performance prediction.

2.4. Section summary

This section discusses the development of white box, black box methodology and numerical methodology for transient performance analysis. The related research work has also been discussed. Table 1 summarizes the advantages and disadvantages of different methodologies. Since the linear model for the white box approach is no longer focused, they are not taken into comparison.

3. Gas turbine transient simulation platform development

The development and application of gas turbine transient simulation, as well as the heat transfer effect, are crucial, but the complexity of the system makes it challenging for researchers to use these methodologies easily. Moreover, launching each simulation from scratch every time is unrealistic. Therefore, easy-to-use software that can simulate gas turbine transient processes is necessary. The development of transient simulation platforms involved three domain techniques: analogue, digital, and hybrid computing. MacIsaac and Saravanamutto offered a parallel comparison of these three technologies [83], concluding that all three simulations were complementary to each other and had their place. Analogue simulations can provide actual time-based results of complex engines but lack accuracy due to presenting non-linear component characteristics. Digital simulations are most suitable for detailed studies, but obtaining real-time results was hard due to slow computer speeds at the time. Hybrid simulation combined the ease of integration of analogue simulation with the logic and stored program capability of digital simulation, but the system was too complex. The development of gas turbine transient simulation platforms will be discussed in this section.

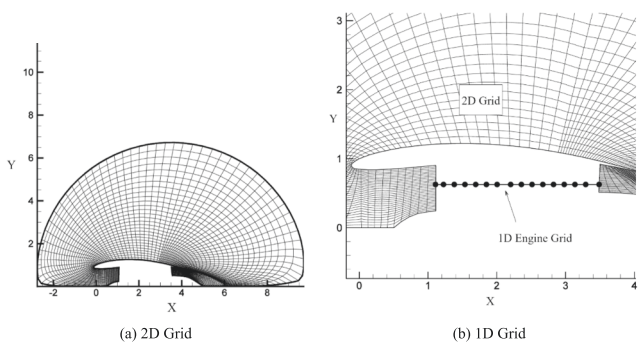


Fig. 9. Computational external and internal grids of the whole engine system [79].

NASA has made significant contributions to the gas turbine performance simulation field by developing several codes, including HYDES, DYNGEN, DIGTEM, DEAN, and others [84–87]. HYDES was a hybrid computer program that investigated the dynamics of one-spool and two-spool turbojet and two-spool turbofan engines using the ICV method. DYNGEN, based on the GENENG method, was the first digital computer program for steady state and transient performance simulation, achieving better accuracy using the modified Euler method [88]. DIGTEM, an advanced version of DYNGEN, was the digital version of HYDES. DEAN improved DYNGEN by implementing pre- and post-processing features [89]. In addition to these codes, NASA has developed Onyx, a Java-based simulation framework that enables direct access to CAD geometry for mesh generation and visualization software tools [90,91]. Onyx was developed as part of NASA's Numerical Propulsion System Simulation (NPSS) project, which integrates various disciplines to enable numerical zooming between 0-dimensional to 1-, 2-, and 3-dimensional component codes [92,93]. In NPSS transient simulation, the Predictor-Corrector method was used. The basic idea of the Predictor-Corrector method is to form a loop. The predictor equation was used to estimate the initial predictor variable, and then the estimated variables were used to calculate the dependent derivative term, which will be used in a corrector equation to form a corrector estimate. The equation converged if the difference between the predictor variable and corrector estimate was small enough. Moreover, the volume dynamic was added to NPSS which filled the gap [94].

In addition to NASA, many other efforts are also being made to develop simulation systems.

Hirst created a program called SYSTRAN, which might be the first analogue computer program [95]. The program improved the unstable regimes in the lumped thermodynamic model created by Saravanamutto. The basic idea was to find equilibrium conditions independently of dynamic stability by programming the model differential equations. Merson's 4th-order Runge-Kutta integration procedure was used to solve the equations.

Cranfield University has also contributed to the development of transient simulation platforms. In 1982, Palmer and Chengzhong developed TURBOTRANS, which enabled transient calculations [96]. The program used Euler's method to replace differential equations with finite difference equations, similar to the method used in DYNGEN. TURBOTRANS introduced "Thermodynamic Bricks" to make the program suitable for different types of gas turbines. Today, TURBOTRANS has been developed into TURBOMATCH, which is suitable for all types of gas turbine transient simulations. TURBOMATCH allows users to choose between ICV and CMF methods for simulation. In TURBOMATCH 3.0, a user-friendly interface has been developed, making it convenient for users to build their gas turbine model. Recently, the heat transfer effect and tip clearance effect has been added to the software.

TRANSEO code was developed by the Thermochemical Power Group at the University of Genoa based on the MATLAB-Simulink environment [97]. TRANSEO code has the capacity to simulate the transient performance of aircraft engines and heavy-duty gas turbines, and in 2000 it had been extended to the microturbine transient cycles. The modularity and flexibility of TRANSEO code enable the simulation of various engine models and the transition of a stationary microturbine to a complete hybrid fuel cell system. The volume dynamic effect is included in the TRANSEO code with the consideration of intercomponent volume.

Chappell and Blevins developed the Advanced Turbine Engine Simulation Technique (ATEST) [98], which is based on a modular approach and is suitable for building arbitrary cycles. ATEST uses the CMF method (an iterative method) during the transient simulation and provides capabilities such as multiple interstage bleed and modelling of second effects during transient, such as tip clearance change and low Reynolds number effects. ATEST 3.0 improved on previous versions with better modelling techniques, component map representations, and other capabilities [99].

Kurzke developed the GasTurb simulator, a commercial gas turbine

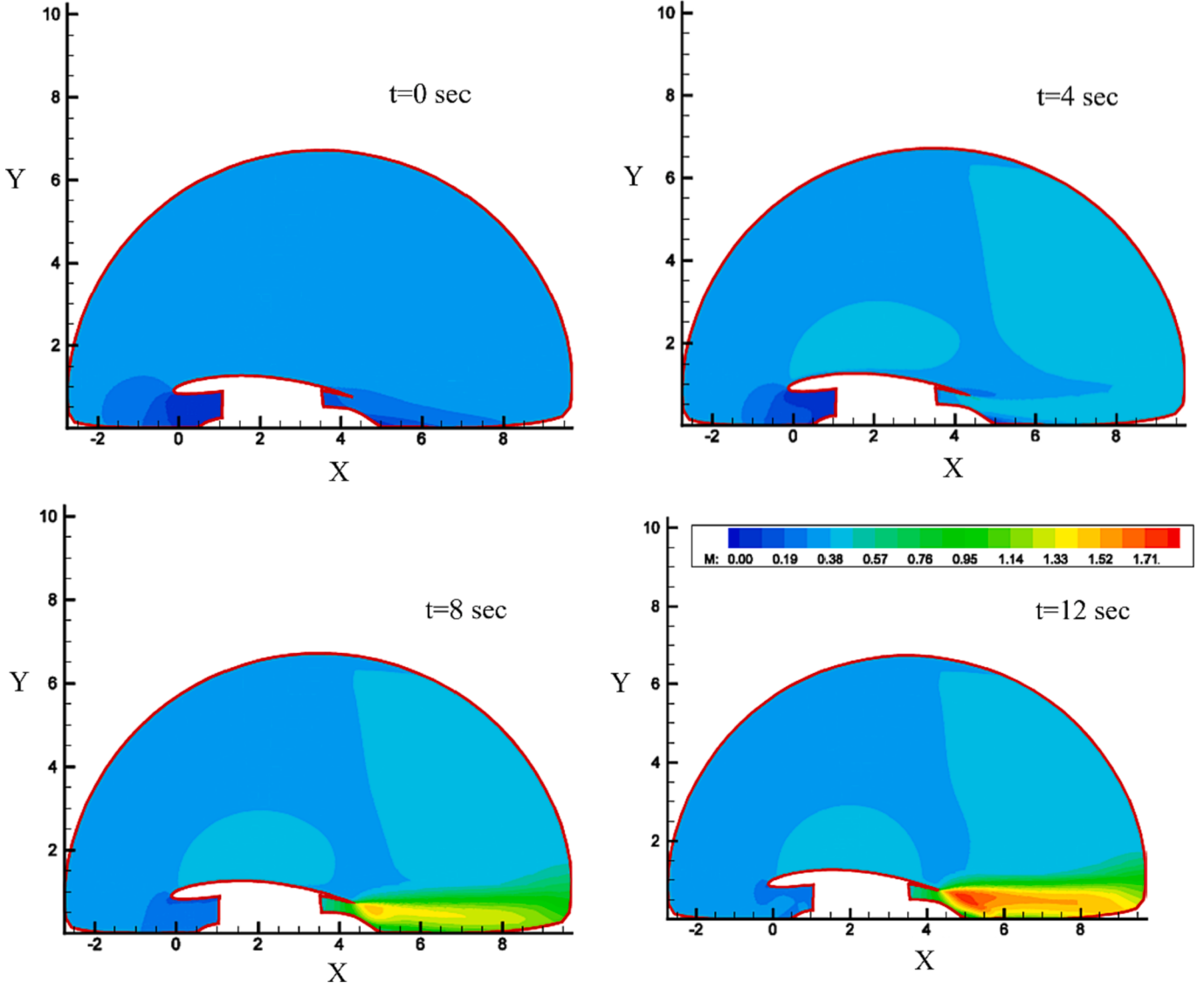


Fig. 10. Mach number contours of the external flow during engine transient [79].

simulator that has been updated to version 14 [100]. It includes several engine models, such as jet engines, gas turbines, propulsion systems, and power generation. In version 14, electric system simulation and afterburner transient were added. Transient simulation offers a choice between a simplified model and an enhanced model. The simplified model uses the CMF method, while the enhanced model includes the heat soakage and tip clearance effects. However, components with heat exchange are simplified to a zero-dimensional model with infinite thermal conductivity and uniform temperature distribution. Transient simulation is only possible after the off-design performance simulation, and the engine model in the library cannot be easily modified.

The GSP, developed by Visser & Broomhead [101], is a user-friendly program designed to improve upon the weaknesses of DYNGEN. It enhances stability, the speed of numerical iteration processes, and the user interface. In GSP transient simulation, conservation equations are solved by a modified Euler Equation. The detailed transient simulation methodology was not illustrated, but the author mentioned that the simulation was calculated iteratively. So, the CMF method might be applied. Different from GasTurb, GSP consists of several component modules or subroutines that allow the user to invoke a single component and make some changes as needed. This provides greater flexibility and a more advanced program architecture. Moreover, heat soakage was taken into

consideration in GSP 11.

Alexiou and Mathioudakis described the use of a generic object-oriented simulation tool called EcosimPro [102]. This tool was then used to develop the Propulsion Object Oriented Simulation Software (PROOSIS) [103]. Due to the fully developed friendly interface, this program was suitable for four levels of users ranging from core library developers to less experienced users who only run simulations using pre-generated customer decks.

Siemens also developed its own gas turbine performance software Simcenter Amesim [104]. However, not much detailed information related to its transient methodology can be found. Based on some researchers' work, the ICV method can be used in Amesim and the component thermal and materials library can be utilized for heat soakage analysis when relevant data is available [105].

4. Heat transfer effects on transient performance

The large temperature difference between the engine metal and the main gas path during the transient process produces a large heat flow, significantly affecting engine performance during and after transient control [40]. As research on gas turbine transient performance prediction continues, discrepancies between simulation and experimental

Table 1
Comparison between different transient simulation methodologies.

	Method	Advantage	Disadvantage
White box approach	CMF [19]	<ul style="list-style-type: none"> Suitable for long time step Suitable for long-term transient simulation Higher accuracy 	<ul style="list-style-type: none"> Only considering the shaft dynamic Unsuitable for complex gas turbine model Long calculation time for complex engine models
	ICV [28]	<ul style="list-style-type: none"> Suitable for complex gas turbine model Considering the volume dynamic effect Faster calculation speed per point Suitable for real-time transient 	<ul style="list-style-type: none"> High requirement on time step choice Map reading problem Lower accuracy compared with CMF Method
	Hybrid [41]	<ul style="list-style-type: none"> Faster calculation speed than CMF method Comparable accuracy compared with CMF method Easy to be implemented 	<ul style="list-style-type: none"> Offset in compressor working line
	PWV [42]	<ul style="list-style-type: none"> Consideration of PW effect 	<ul style="list-style-type: none"> Significantly increased calculation time
	IMF [44]	<ul style="list-style-type: none"> No map reading problem 	<ul style="list-style-type: none"> Relative lower accurate Unknown time step choice and calculation speed
	Advanced [81,82]	<ul style="list-style-type: none"> Capability of estimating rotating stall and surge Higher accuracy 	<ul style="list-style-type: none"> Unknown time step choice and calculation speed
Black box approach	MLP [48]	<ul style="list-style-type: none"> Simple and easy to train 	<ul style="list-style-type: none"> Long training time compared with RBF
	RBF [54]	<ul style="list-style-type: none"> Relatively higher accuracy compared with MLP Low requirement on the number of hidden layers Short training time 	<ul style="list-style-type: none"> Higher training requirement
	NARX [58,60]	<ul style="list-style-type: none"> High capability More suitable for dynamic condition Higher generalization capability 	<ul style="list-style-type: none"> Longer training time and more complex structure compared with static network
Numerical Approach	CFD [78, 79]	<ul style="list-style-type: none"> 2D external flow field demonstration Direct flow field estimation No map reading problem 	<ul style="list-style-type: none"> Lower-order model for the core engine High computational cost High geometry information requirement

results have led to the identification of heat transfer effects that affect the transient operation of engines. Heat transfer effects refer to the effects coming from the heat exchange during the gas turbine transient process, including the heat soakage effect, tip clearance effect, and component characteristic change effect. Heat soakage is the process of heat transfer between the working fluid and the engine component, while the tip clearance effect results from changes in clearance due to temperature, centrifugal force, and pressure difference. Component characteristics are described by the component map, which can be affected by changes in working flow physics. An illustration of the heat transfer effects on the performance of the components is shown in Fig. 11. A brief introduction to the heat transfer effect was provided by

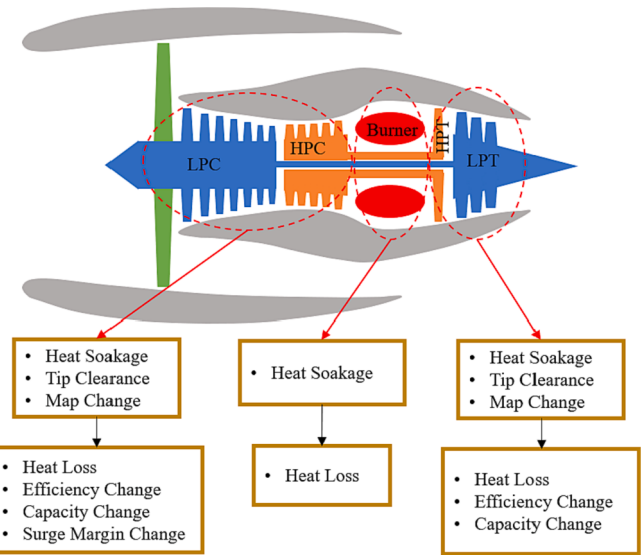


Fig. 11. Heat transfer effects on the performance of the components.

Hashmi et al. [8]. MacCallum used the term 'thermal soak' to summarize the effects, which refer to the performance difference from the equilibrium performance after rapid acceleration and deceleration [10]. These effects significantly influence the engine acceleration or deceleration time and the rate of change of aerothermodynamic parameters [106].

This section will discuss the heat soakage, tip clearance, and component characteristic change effects separately. The methodology development and application will also be included.

4.1. Heat soakage effect

When investigating gas turbine steady-state performance, it is reasonable to assume that the compression and expansion process occurs adiabatically because the heat flows are exceedingly small compared to engine component powers [40]. However, during the transient manoeuvre, the heat transfer between the primary gas path and engine components is too big to ignore and will affect component performance. The large temperature leads to a large heat flux, which can lead to non-adiabatic expansion and compression both during and after a transient manoeuvre [10]. Also, some engines can consume a typical additional 30% energy excess to reach a new higher steady state operating temperature due to the thermal soakage [1]. According to the research findings, it was discovered that heat soakage causes a delay in the transient response of gas turbines. Specifically, during the acceleration phase, there is a reduction in the rate of increase of engine thrust and shaft PCN. Conversely, during deceleration, the rate of decrease is reduced. In this section, the methodology development of heat soakage analysis and the effect of heat soakage on gas turbine performance will be discussed.

The significance of the heat soakage effect was first mentioned in 1968 by Bauerfeind [107], who simulated a two-spool turbofan engine to introduce the heat soakage effect. Additionally, MacCallum identified the transient factors that may impact the performance of a simple jet engine after rapid acceleration [10]. To analyse the effect of heat absorption, he utilized the F parameter as a correction factor for the polytropic efficiency. The F parameter was determined as the ratio of the heat transferred from the air to the work transferred from the air. The impact of the F parameter on the adiabatic compression and expansion equation is shown in Eq. (20),

$$\frac{P_2}{P_1} = \left(\frac{T_2}{T_1} \right)^{X/(1-F)} \quad (20)$$

where P_1 and P_2 are the total pressures at the start and end of the process. T_1 and T_2 are the total temperature at the start and end of the process, X is the polytropic index of compression or expansion, and F is the ratio of the heat transferred from the air to the work transferred from the air.

The F parameter method can predict the heat absorption effect, but it is more of an empirical formula for polytropic efficiency modification. To improve the simulation, the lumped parameter method (LPM) for heat soakage calculation was introduced to gas turbine transient simulation by Fawke and Saravanamuttoo [108]. The mean temperature based on the component inlet and outlet temperature is used to determine the values of the Prandtl number, thermal conductivity, and viscosity for the gas to calculate the heat transfer coefficient (HTC). However, for each component, only one HTC value is applied, making the investigation of the heat soakage affect an approximation. Based on the simulation outcomes for acceleration and deceleration, it was found that the operating path of compressor characteristics had not been significantly affected. Khalid and Hearne provided a full description of the LPM in their transient performance heat soakage model, which was used to investigate the heat absorption effect on a two-spool turbofan engine. [109]. Eqs. (21)–(24) illustrated the process of the LPM,

$$\tau = m^* C_p / (h^* A) \quad (21)$$

$$T_m^{t+\Delta t} = T_g^t - \left(T_g^t - T_m^t \right)^* e^{-\frac{\Delta t}{\tau}} \quad (22)$$

$$q = -h^* A^* \left(T_m^{t+\Delta t} - T_g^{t+\Delta t} \right) \quad (23)$$

$$T_{out} = T_{out,ad} - \frac{q}{m^* C_p} \quad (24)$$

where τ is the time constant, m is the mass of the metal, h is the HTC, A is the wetted area, T_m is the metal temperature, T_g is the main gas temperature, q is the heat flow rate, T_{out} is the component exit total temperature, and $T_{out,ad}$ is the component exit total temperature under the adiabatic condition. The basic idea of LPM is that the interior temperatures of bodies remain essentially uniform at all times during a heat transfer process. During the process, the heat absorption of compressors and turbines was taken into consideration, except for the combustor. They also considered the effect of turbine cooling flow variations, control temperature sensor response and tip clearance variations, which will be discussed in subsequent sections.

To make LPM more realistic, Kim raised a ‘heat transfer correction factor (HTCF)’ to modify the heat soakage effect during transient [110]. The equation of heat transfer correction factor A is shown in Eq. (25), where a and c are constant in equation, D is characteristic diameter, k is thermal conductivity, L is characteristic length.

$$HTCF = a^* D^c * \frac{k}{L} \frac{A}{m^* C_p} = Constant \quad (25)$$

where a and c are constant in equation, D is characteristic diameter, k is thermal conductivity, L is characteristic length, and A is the wetted area.

LPM offers a convenient way to simulate the heat transfer between the solid and fluid. However, it assumes that the fluid temperature keeps constant during the heat transfer process, leading to overestimating the heat flux. Naylor moved the LPM a step further by considering the fluid temperature change during the heat transfer process [40]. The improved LPM is shown by Eqs. (26)–(30).

$$Q = U((T_{f0} - T_{m0})/Z)(e^{Z\Delta t} - 1) \quad (26)$$

$$U = 1/(1/(h^* A) + 1/(k^* A/X)) \quad (27)$$

$$G = W_f^* \Delta t^* C_p f \quad (28)$$

$$M = M_s^* C_p s \quad (29)$$

$$Z = -(U/G + U/M) \quad (30)$$

where Q is the quantity of heat transferred during the time interval, T_{f0} and T_{m0} are temperatures of fluid and solid at the start of the time interval, U, G, M, Z are the thermal characteristics of the system, X is the distance from wetted area to solid centre of mass, W_f is the working fluid mass flow rate, and M_s is the material mass. This method could modify the fluid temperature during the heat transfer process and offer a much more accurate outcome. Besides, Naylor also developed the stream method. Components were divided into several discrete solids to apply the stream method, each with their own wetted surface, as shown in Fig. 12. The temperature of the fluid leaving the current surface was used as the temperature of the fluid entering the next surface, and so on, until the fluid left the solid completely. Compared with the original LPM, the stream method was more stable and could handle the calculation when neither fluid nor solid could be assumed to be a temperature reservoir and where conduction is significant.

The stream method improved the original LPM. But it needed a specific gas turbine component structure to build the model. So, a thermal network model was developed by Visser and Dountchev to offer a more generic heat soakage estimation [111]. In the thermal network, several heat sinks represented the components. Each heat sink was calculated by the LPM method and then connected using Non-linear Differential Equations. With the link among each heat sink, the original 0-D thermal recuperator model can be seen as a quasi-1D model (in radius direction). However, this method had the same limitation as the original LPM. It could not represent the heat transfer process inside parts, and there would still be errors for complex heat transfer patterns.

The stream method and the thermal network improved the LPM. However, the heat calculation between the surface to surface is still discontinuous. A real 1D method is still needed. Zhuojun fulfilled this gap by extending the original 0D method in the axial direction [44]. In the 1D method, each solid component was no longer treated as one point located at the centre of mass. By using the integral method, the temperature distribution along the component could be simulated with much more accuracy. However, temperature profile, area, and mass distribution along the length of turbomachinery were considered linear, which was inconsistent with the fact.

The finite element method (FEM) was introduced by Chapman et al. to estimate the heat transfer rate between the HPT shroud, as well as the disc, and the working fluid [112,113]. Compared to the LPM, the finite element method provides a more detailed representation of the internal temperature distribution and can be applied more easily to components that consist of two materials. The heat equation is described by Eq. (31)

$$\frac{\rho^* C_p^* \partial T}{k} = \frac{\partial^2 T}{\partial X^2} \quad (31)$$

The central forward finite difference method was utilized when solving partial differential equations.

Both the LPM and FEM have their advantage. Progress had been made by creating a quasi-one-dimensional heat transfer model that combined both LPM and FEM by Chen et al. [114]. In this new model, the internal nodes in FEM had been replaced with lumped engine components, such as a lumped compressor stage or a lumped combustor. This allowed for the consideration of all engine components with proper settings. Additionally, the new internal nodes could account for heat conduction and radiation, whereas the original LPM only considers heat convection.

The methodology mentioned above can be concluded as the replacement structure model (RSM) [115] because the idea is to use mathematical equations to represent the components in the gas turbine. However, there are two other models: the impulse response model (IRM) and the state-space model (SSM). The idea of IRM is to calculate the impulse response $g(t)$ when subjected to a unit impulse input. For the SSM, the idea is to calculate the temperature change using the state equation. Riegler proposed an IRM-based method whereby primary gas

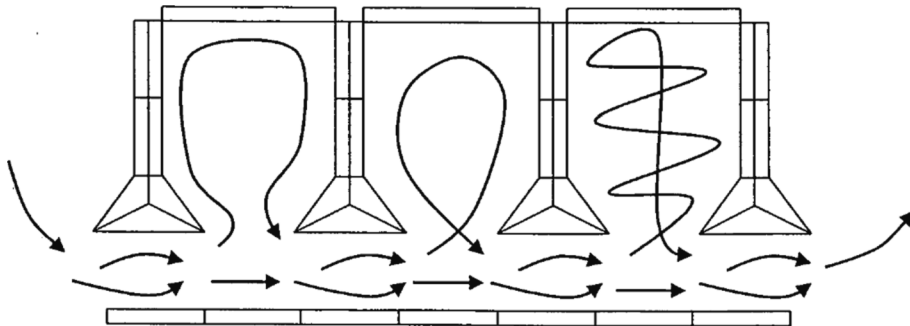


Fig. 12. Illustration of a streams method model of a multistage disc cavity [40].

path heat soakage is calculated non-dimensionally using Biot and Fourier numbers[116]. The governing equation can be described by Eq. (32),

$$q/(k^* \Delta T^* L) = f(Fo, Bi, shape) \quad (32)$$

The method describing heat transfer phenomena depends linearly on temperature. Therefore, steady-state and transient phenomena might be modelled separately, and the effects might be superimposed. However, Naylor pointed out that the workings of the method presented were still based on Nusselt numbers for flow through tubes, mean component inlet and outlet temperatures, and mean component temperatures [40]. Merkler et al. developed an SSM-based model for disc temperature calculation [115]. The governing equation is shown in Eqs. (33)–(35)

$$T_{m,new} = A*T_{m,old} + B*T_g \quad (33)$$

$$u = C*T_{m,old} + D*N \quad (34)$$

$$\sigma = E*T_{m,old} + F*N \quad (35)$$

Where A to F are matrices, and u and σ are functions of time. Both IRM and SSM have their advantage. However, after a comprehensive review, it shows that the RSM is the best popular model since it directly indicates the physical process during the heat transfer process.

After discussing the heat soakage calculation, it is necessary to discuss the heat soakage effect on component performance. A common way was to assume that the compressor and turbine were still working at the adiabatic condition [117]. Part of the heat transfer occurred before the adiabatic component process, and the rest occurred after the adiabatic component process. This would only affect the component inlet and outlet temperature instead of modifying the component power [118]. However, some researchers believe that the heat transfer process will affect the compressor and turbine power [111,119]. And a modification of the component power should be included. The corrected component power and component outlet enthalpy are estimated by Eqs. (36)–(38)

$$PW_{corr_compre} = \left(\frac{h_{out}}{h_{in}} - 1 \right) * \frac{q}{\eta_{is}} * R_q \quad (36)$$

$$PW_{corr_turbin} = \left(\frac{h_{out}}{h_{in}} - 1 \right) * q * \eta_{is} * R_q \quad (37)$$

$$h_{out} = (h_{in} * W_{in} + Q + PW + PW_{corr}) / W_{out} \quad (38)$$

where PW is the correct power for the compressor and turbine, η_{is} is the isentropic efficiency of the compressor and turbine, R_q is the inlet/exit heat transfer ratio, and Q is the quantity of heat. Based on these equations, the modified outlet enthalpy can be estimated and used to modify the transient component performance.

The above discussion illustrates the development in heat soakage methodology development. Significant progress had been made to

improve the accuracy during the heat transfer calculation. However, since the LPM offers a convenient way to simulate the heat transfer between the solid and fluid, it has been used in extensive research. Zhili and Kuo developed an unstable heat exchange model being used in gas turbine transients [120]. The difference between their work and Khalid and Hearne's work was the choice of HTC. In Khalid and Hearne's investigation, only turbulent flow was considered. But both the laminar flow and turbulence flow were considered in Zhili and Kuo's work. Unfortunately, they didn't compare their outcome with the experiment data. In 2001, Stamatidis and Mathioudakis also included the heat transfer effect in their real-time engine model [121]. LPM was being used, but the choice of HTC was different. However, the LPM was only applied to the compressor and turbine blades and casings for simplification. Hu and Xiaochun applied Khalid and Hearne's on a different gas turbine engine [122]. With the same simulation environment, they compared their outcome with Maccallum's work, and it showed that the LPM had a better prediction than the F parameter method. Tagade developed a gas turbine simulation model for the startup to shutdown process of a twin-spool turbofan engine [123]. The model takes into account thermal transients, shaft transients and gas dynamic transients. In the thermal transient simulation, LPM is used. Alves and Barbosa built a regenerative-cycle gas turbine model that considered friction and non-adiabatic volumes [124]. The importance of the heat soakage effect in the micro-turbine engine was mentioned by Davison and Birk [125,126]. The engine model was validated against the experimental data. Although there were overestimations in the transient performance, the correlations were good. The heat soakage model was closer to the experimental data compared with the CMF model. Qiuye used the lumped parameter method to analyze a two-spool engine transient performance [118]. Their work was similar to Zhili's, but they moved one step further to compare the simulation results with experimental data. Besides, they correct the Nusselt number of compressor blades by taking both laminar flow and turbulence flow into consideration. Vieweg introduced the transient heat soakage code within the DLR's in-house gas turbine simulation framework GTLab and compared the outcome with the engine data [117]. The code uses the lumped parameter method but improves the method by using a scaling process to avoid manually updating the HTC. With that, only the design point needs to be estimated by the user. Then, the heat soakage code was extended to allow for heat transfer among different components, bleed flows, and the environment [127]. Ferrand investigated the turboshaft engine power losses caused by heat soakage in the combustion chamber [128]. However, with the method developed, there is only a maximum correction of 0.55% of the design speed, which shows that it is not sufficient to correct the heat soakage effect only considering the combustion chamber. Kim et al. developed a simulation tool for the dynamic behaviour during the start-up of heavy-duty gas turbines [129]. They adopted a multi-segment model instead of using a single control volume model where the compressor was calculated group by group and the turbine was calculated stage by stage. Besides, they used iterative calculations at each control volume to have a more accurate outcome.

In conclusion, the heat transfer calculation between components and the working fluid has evolved from a 0D to a quasi-1D model. However, the LPM remains popular due to its simplicity. Further analysis of the heat transfer effects on component performance is still necessary, as different researchers hold differing opinions. Table 2 concludes the advantages and disadvantages of the different heat transfer estimation methodologies mentioned above.

4.2. Tip clearance effect

During transient manoeuvres, gas turbines are expected to experience varying thermal and mechanical loading that can lead to small changes in the axial and radial dimensions of the components. These changes are caused by three main reasons: (1) The thermal growth due to the change in component temperature; (2) The centrifugal stresses on the rotating components; (3) The pressure stresses on the static components. An illustration is shown in Fig. 13. In this section, progress in tip clearance prediction and component performance modification will be discussed.

When estimating thermal growth, it is strongly linked with the heat transfer calculation that was discussed in Section 4.1. Based on the discussed LPM, each component was treated as a node with the mass at the centre of it, and the component temperature was known at each time interval [40]. It is easy to apply the thermal expansion equation to the lumped component. The thermal expansion equation is shown in Eq. (39),

$$u = a^*L^*(T_m - T_{ref}) \quad (39)$$

where u is the thermal growth, a is the expansion coefficient, and T_{ref} is the temperature of components at the reference point. With the setting of the reference point, the deflection due to the temperature change can be estimated [130]. Progress had been focused on the development of a more accurate mean temperature prediction method. Kypuros et al. established a 1-D analytical method to have a better mean temperature prediction on the temperature distribution along the rotor width direction and the casing radius direction [131,132]. FEM was used by Pilidis and MacCallum to develop a model for blade tip movement as well as seal clearance change [133]. The model represented a deep disc rotor with three elements: a thick hub, a thin diaphragm and an outer section or rim. Naylor applied the same idea to his ring method when calculating the disc radius change [40]. In the ring method, the disc was divided into small rings (typically 5 to 6 rings), and the overall radius change was the sum of the displacement of all the small rings. MacCallum developed a 2D disc temperature distribution model [134]. The geometry of the disc has been divided in the radial into 20 increments and then in the axial direction into 10 elements. The effect on the choice

of the number of elements had also been studied, and it was found that the change in the average temperature was under 1 K when increasing the axial elements to 14. Chapman et al. established a 1-D FEM model to predict the thermal displacement of the turbine shroud (along the radius direction) and rotor (along the thickness direction) [112,135]. Sheng et al. improved the thermal expansion model by considering the temperature-dependent heat expansion coefficient and made the simulation time suitable for real-time transient simulation [136].

Instead of using the mean temperature for thermal displacement estimation, it can be estimated directly based on the temperature field. Fang et al. derived the basic equation of the temperature field of uniform thickness and single rotor disk and then it was used to estimate the thermal expansion by integration [137]. The equation is shown in Eqs. (40)–(41),

$$T = T_a + (T_1 - T_{a1}) \frac{K_1(x_0)I_0(x) + I_1(x_0)K_0(x)}{K_1(x_0)I_0(x_1) + K_0(x_1)I_1(x_0)} \quad (40)$$

$$u = a^*L^* \int (T - T_{ref}) dx \quad (41)$$

where T is the disc temperature at different radii, T_a is the cooling flow temperature at different radii, T_1 is the temperature at the rim, T_{a1} is the cooling flow inlet temperature, $K_0(x)$ and $I_0(x)$ are two particular solutions of the zero-order Bessel equation. Compared with the original thermal expansion method, this method considered the temperature difference along the disc radius. However, the calculation process was much more complex since it needed to solve the Bessel equation.

Another way is to express thermal displacement as an exponential function of time. It was known that the component temperature could be expressed as a function of time. Since the thermal growth of the component was directly proportional to the component temperature, it was able to express the thermal growth as an exponential function of time [109]. Khalid and Hearne then estimated the thermal growth of each component by using Eq. (42).

$$\Delta R_{j,trans,t+\Delta t} = \Delta R_{j,ss,t+\Delta t} - (\Delta R_{j,ss,t+\Delta t} - \Delta R_{j,trans,t}) * e^{-\frac{\Delta t}{\tau}} \quad (42)$$

where $\Delta R_{j,trans,t+\Delta t}$ is the transient changes in radius at the end of the time interval, $\Delta R_{j,ss,t+\Delta t}$ is the steady state change in radius at the end of the time interval and $\Delta R_{j,trans,t}$ is the transient changes in radius at the start of the time interval. With the estimated thermal expansion, the total tip clearance change can be estimated with the consideration of centrifugal stress and pressure stress.

The displacement caused by centrifugal force is also important during the tip clearance estimation. Two components are considered. One is the rotor blade, and the other is the disc. For the blade, a common simplification was that the blade was assumed as a constant cross-area flat plate [39]. Fang et al. improved the estimation method by considering a changing cross-section area blade [138]. Instead of the changing cross-section area, the effect coming from the shrouded turbine blade was taken into consideration by Naylor and Pilidis [39,40]. For the rotating disc, the centrifugal deformation will be affected by the disc's mass and the centrifugal force from the blade mass. When considering the disc displacement due to its mass, it is commonly assumed that the disc has a unique thickness [137]. When applying this method during the disc displacement due to centrifugal force, it was suggested that the thickness of the disc should be equal to the minimum diaphragm thickness of the actual disc profile [39]. The displacement due to blade mass was not considered by Kypuros et al. and Chapman et al. and it was mentioned that this force would lead to a 15.9% difference when estimating the tip clearance movement [136].

The pressure forces will lead to a change in the casing radius [131]. However, pressure deformation is relatively small compared to the effect from thermal deformation and centrifugal deformation. In some cases it was assumed negligible and was not introduced to the calculation [119].

Research showed that the change in tip clearance will affect

Table 2
Comparison between different heat transfer estimation methodologies.

Method	Advantage	Disadvantage
F parameter [10]	• Direct performance modification	• Relative low accuracy
LPM [109]	• Easy to be implemented	• Neglection of fluid temperature change Neglection of material internal thermal resistance
Stream [40]	• Easy to be implemented Consideration of fluid temperature change	• Neglection of thermal resistance
FEM [112,113]	• Consideration of the thermal resistance Suitable for complex structure	• Long calculation time High requirement on calculation time step
IRM [116]	• High accuracy	• Low Transparency Long calculation time during transient simulation
SSM [115]	• Short calculation time	• High cost of modelling

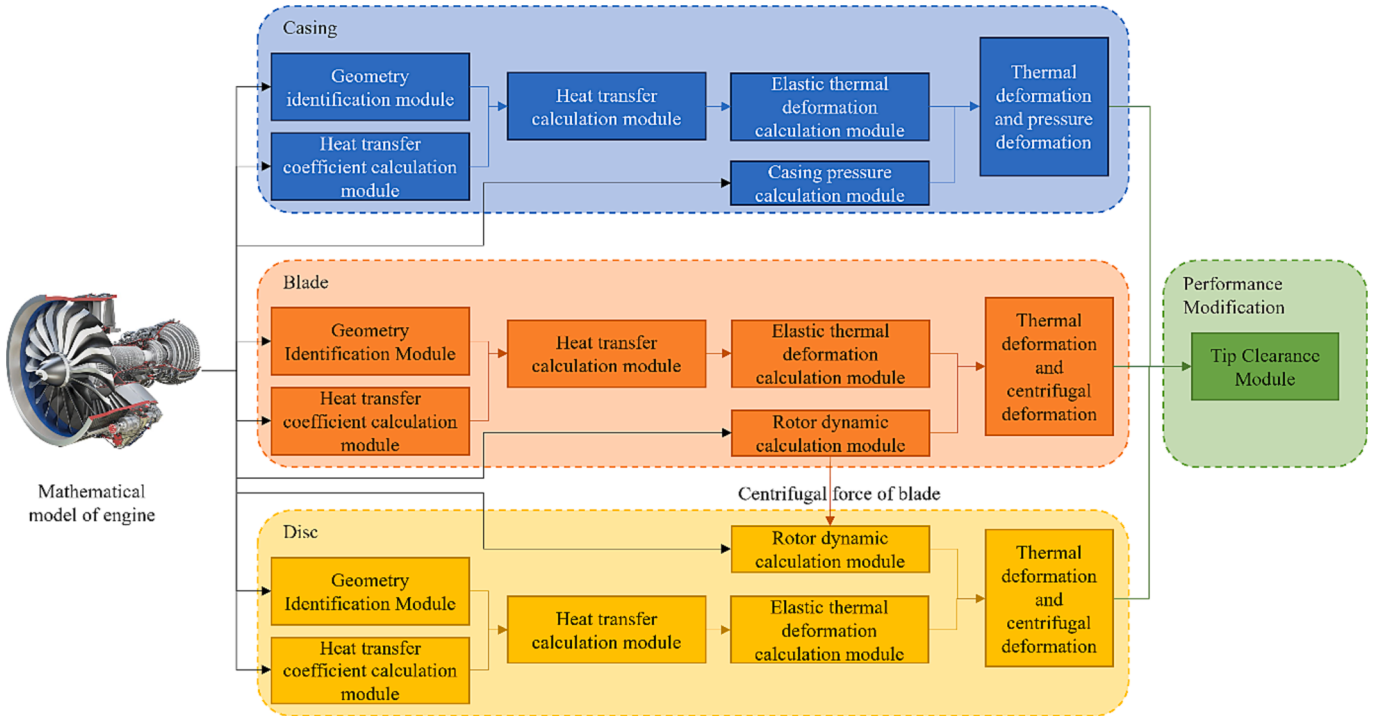


Fig. 13. Structure of tip clearance estimation during engine transient.

component efficiency, mass flow, and surge margin [139]. Several researchers had investigated the relationships between tip clearance and component efficiency. The modification methodology on the tip clearance effect and be concluded in two ways. The first is the empirical correlation modification, and the second is the direct modification.

The idea of the empirical correlation modification method is to use the empirical correlation and tip clearance value to modify the component performance. In 1970, Lakshminarayana derived an expression for the decrease in compressor efficiency due to the tip clearance change, which is expressed by Eqs. (43) [140].

$$\Delta\eta = \frac{0.7\lambda\psi_*}{\cos\beta_m} \left[1 + 10\sqrt{\frac{\phi}{\psi} \frac{\lambda A}{\cos\beta_m}} \right] \quad (43)$$

where η is efficiency; λ is nondimensionalized clearance; ψ is blade loading coefficient; β_m is mean air angle; ϕ is flow coefficient; A is the aspect ratio of the blades. The turbine efficiency modification methodology was raised by Baskharone [141]. The correlation is shown in Eq. (44)

$$s_Eff_{TC} = 1 - K^* \left(\frac{TC - TC_{ref}}{l_b} \right)^* \left(\frac{r_{rototip}}{(r_{rototip} + r_{rotorhub})/2} \right) \quad (44)$$

where s_Eff_{TC} is the turbine efficiency scaling factor, K is an index defined as $K = 1 + 0.5(\psi_{Ztip}^{3.36})$, TC is the tip clearance absolute value, TC_{ref} is the tip clearance reference value, r is the radius, and ψ_{Ztip} is the Zweifel loading coefficient. This method had been used by several researchers. Hongmei and Zhili utilized Eq. (43) during the tip clearance change in their transient study [142]. Jiaomei also investigated the tip clearance movement and its effect on engine transient performance using Eq. (43). [143]. But only the last stage of the compressor was considered during the performance modification. An irregular finite volume mesh method for the disc that has universality was developed by Ma [144]. Eq. (44) was used during the performance modification. However, this method was finally applied to a transient simulation as a post-modification, and it might lead to an error since the transient performance will be affected by tip clearance change during the process

and might lead to a different working line.

The empirical correlation can offer a relative accuracy modification. However, it is hard to use when a certain blade profile is missing. Direct modification method is then recommended under this condition. MacCallum found that the change in compressor tip clearance caused a reduction in efficiency of 0.4%, and the change in seal clearance caused an increase in the cooling flow of 0.2% [10]. Walsh and Fletcher suggested that a 1% increase in tip clearance will lead to a 1–2% reduction in efficiency and a 2–15% reduction in surge margin [1]. Hourmouziadis and Albrecht suggested that the exchange rate is in the range of 2% (a 1% increase will result in a 2% decrease in efficiency) [145]. Shirzadi and Saeidi suggested that the exchange rate is in the range of 0.8% based on turbine polytropic efficiency [146]. This method is also applied in GasTurb, where the user can directly set the ratio between the change in clearance and the change in component performance [119].

4.3. Component characteristics change effect

Changes in clearance and heat absorption can also affect the characteristics of engine components. The exchange of heat between the main gas path and the components changes the temperature of the gas path, leading to modifications in the development of the boundary layer and fluid density [147]. Furthermore, changes in tip clearance can impact component characteristics, including compressor efficiency and surge margin.

The ‘bulk’ effect on compressor characteristics caused by density change was first investigated by MacCallum [148]. It was found that a reduction in air density at the compressor outlet led to a decrease in the compressor surge margin. Later, Grant reported that heat transfer from the wall to the boundary layer affects the development of the boundary layer, accelerating separation [149]. MacCallum and Grant developed a method to predict the effects of boundary layer changes due to heat transfer on the characteristics of an axial-flow compressor [150]. The method included a predicted mean line method for compressor characteristic map generation and an empirical correlation for modification. They found that the thickening of the heated compressor blade boundary layer was more significant on the suction surface than on the

pressure surface, causing a blockage effect (shown in Fig. 14). They also proposed an empirical correlation for the change in flow outlet angle with respect to temperature change, as shown in Eq. (45).

$$\frac{\Delta\alpha_2}{\epsilon^*} = \Delta T^* \left(0.0005 + 0.00084 \frac{i - i^*}{\epsilon^*} \right) \quad (45)$$

where $\Delta\alpha_2$ is the deflection angle as shown in Fig. 10, ϵ^* is the designed deflection, ΔT is the temperature difference between the blade aerofoil temperature and adiabatic wall temperature, i is the incidence angle, and i^* is the design incidence angle. Notably, the angle of departure had doubled compared to the adiabatic case due to the rapid growth of the suction surface boundary layer. The method provided a predicted output, but no experimental data was presented to confirm the theoretical predictions [151]. Also, they did not explain their predicted mean line method in detail, nor how $\Delta\alpha_2$ effect the performance map.

Further work was done by MacCallum and Pilidis by developing compressor map modification empirical correlations for speed line and surge line modification [147,152,153]. Equations for the corrected speed of the compressor and the movements of the surge pressure ratio are expressed by Eqs. (46)–(47).

$$\frac{\Delta N}{N} = C_1 \frac{T_b - T_{air}}{T_{air}} + C_2 \frac{Q}{m^* C_p^* T_m} - C_3 \frac{\Delta(\delta)}{g} \quad (46)$$

$$\frac{R_{ht} - 1}{R_{ad} - 1} = 1 + C_4 F - C_5 \frac{\Delta(\delta)}{g} \quad (47)$$

where the coefficients C_1 , C_2 , and C_3 represent the changes due to movements of the aerofoil boundary layer, changes in the fluid density and changes in the blade tip clearances, respectively, δ is the tip clearance, g is the staggered gap between blades, R is the surge margin, coefficients C_4 and C_5 represent the changes due to density changes of the fluid and the tip clearances, respectively. This program was then used to analyze the compressor surge margin movement of a two-spool bypass engine during transient [154]. For the LPC, the values for C_1 and C_3 were select as -0.07 , -0.07 and 0.3 . For the HPC, the value for C_1 and C_3 were select as -0.1 , -0.1 and 0.3 . This similar method was then be used by Stamatis which allowing the evaluation of the effects related to heat transfer to the turbine blades on its performance characteristics [155]. In his research, he considered the effects of thermal dilatation and boundary layer development and then corrected the turbine map based on them. Besides, the blade temperature took the consideration of nonuniform temperature distribution which will offer a better outcome for the turbine blade. The movement of the compressor speed line is shown in Fig. 15.

Larjola investigated the effects of heat transfer on both compressor surge margin and turbine mass flow blockage [156]. His work found that changes in the boundary layer and air density were responsible for 66.2% of total surge margin reduction, while clearance change accounted for only 0.02%. Larjola's prediction method had better accuracy than MacCallum and Grant's, as it considered surge line movement. In the same year, Crawford and Burwell attempted to experimentally confirm MacCallum and Grant's findings [151]. Using experimental data from several "Bodie" transient events, they calculated the total temperature and steady-state adiabatic efficiency of the unsteady compressor during the process from take-off power to rapid

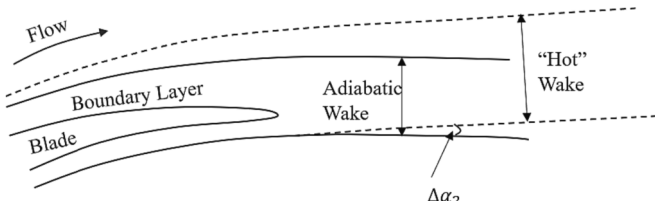


Fig. 14. Change in boundary layer development due to heat transfer [150].

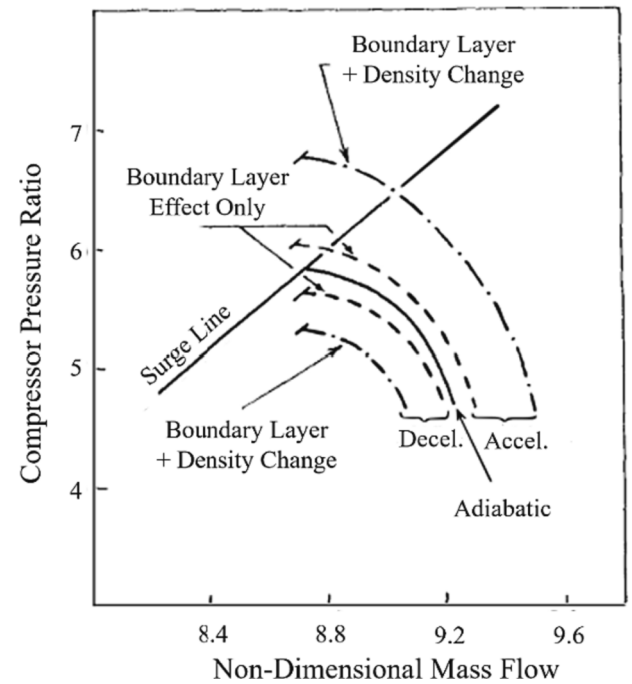


Fig. 15. Compressor speed line movement due to boundary layer effect and density change [147].

deceleration and immediate re-acceleration after idling. Although they found no statistical correlation between stall margin loss and heat flow, they observed that average heat flow was greater when the compressor stalled.

Torella investigated the secondary transient effect (heat transfer, packing lag in the ducts, transient effect in the combustion) [157]. Expressions were derived to evaluate the variation of the compressor and turbine efficiencies, shown in Eqs. (48)–(49).

$$\text{Compressor : } \frac{\Delta\eta_c}{\eta_c} = \frac{\frac{T_{on}}{T_o} - 1}{\frac{T_{on}}{T_o} - 1 - 0.5 \frac{\Delta T_{on}}{T_o} \ln \frac{T_{on}}{T_o}} \quad (48)$$

$$\text{Turbine : } \frac{\Delta\eta_t}{\eta_t} = \frac{\ln \frac{T_{on}}{T_o}}{2(\frac{T_{on}}{T_o} - 1)} \frac{\Delta T_{on}}{T_o} \quad (49)$$

where T_{on} is the component exit temperature, T_o is the component inlet temperature and ΔT_{on} is the temperature drop due to the heat transfer. Since the change in components efficiency was determined by exit temperature while the exit temperature depended on the efficiency, an iterative procedure was necessary.

In 2007, Morini analysed the heat soakage effect on the compressor by using a simple method based on an equivalent variation of the compressor polytropic efficiency [158]. They concluded that the heat soakage has a high impact at low shaft speed and negligible impact close to nominal shaft speed. In the same year, Shah analysed the heat transfer effect on compressor performance [159]. He raised the idea of non-dimensional heat flux which was a heat transfer rate that had been normalized by the blade inlet stagnation enthalpy inflow rate. Then he concluded the correlation of total pressure change coefficient and change in flow angle deviation with the nondimensional heat flux, which is shown in Eqs. 50–51.

$$\Delta\delta = \frac{q^*}{0.01} * \zeta, \text{ where } \begin{cases} \zeta = 0.1^\circ \text{ for } M = 0.4 \\ \zeta = 0.25 \text{ for } M = 0.8 \end{cases} \quad (50)$$

$$\Delta\omega = \frac{-\Delta P_t}{P_t} \frac{P_t}{P_t - P_s} = \frac{1}{1 - (1 + \frac{r-1}{2} M^2)^{\frac{1}{r-1}}} \frac{\gamma M^2}{2} q^* \quad (51)$$

where $\Delta\delta$ is the change in flow angle deviation, q^* is the non-dimensional heat flux, M is the Mach number, $\Delta\omega$ is the change in blade row total pressure loss. In 2015, Kiss and Spakovszky used Shah's correlation to analyse the effect on compressor stall margin during a re-acceleration phase of a Bodie manoeuvre [160,161]. To illustrate the non-adiabatic transient, they developed the "composite compressor map" that includes the time-dependent speed line, stall line and working point. Fig. 16 illustrates a comparison between the original compressor map with the composite compressor map, where the map in black represents the former and the map in colour represents the latter. τ in Fig. 16 represents the non-dimensional time, which equals t/t_{acc} . Besides, the model they created also included stage re-matching and deviation effects, which are not included in current software like NPSS. Compared with the NPSS, the new model captured an 8.0-point stall margin loss when NPSS is 1.2-point. However, this method calculates the heat transfer rate q^* based on the component temperature (based on steady-state operating point) and the flow field temperature (based on adiabatic Bodie transient) in advance. So, the heat transfer rate is not calculated during the transient operation. This led to some errors in the calculations, but the magnitude has not been analyzed.

Zhuojun also analysed the component characteristic change in his work [162]. The map update method was similar to the work of Pilidis and MacCallum. However, the new method enabled the characteristic map to be updated at each time interval with the updated scaling factor of mass flow, pressure ratio and efficiency.

A brief description of the different methodologies described above and a comparison among them is shown in Table 3.

4.4. Section summary

In this section, various methodologies applied to simulate heat transfer effects on gas turbine transient performance are discussed. Three aspects are considered: heat soakage, tip clearance change, and component characteristic change. Heat soakage models have progressed from 0D to quasi-1D models, although the 0D model remains popular due to its convenience. For tip clearance change due to heat expansion, the calculation logic still relies on the simple thermal expansion equation. In terms of component modification, there is no unified understanding among researchers, and different opinions exist.

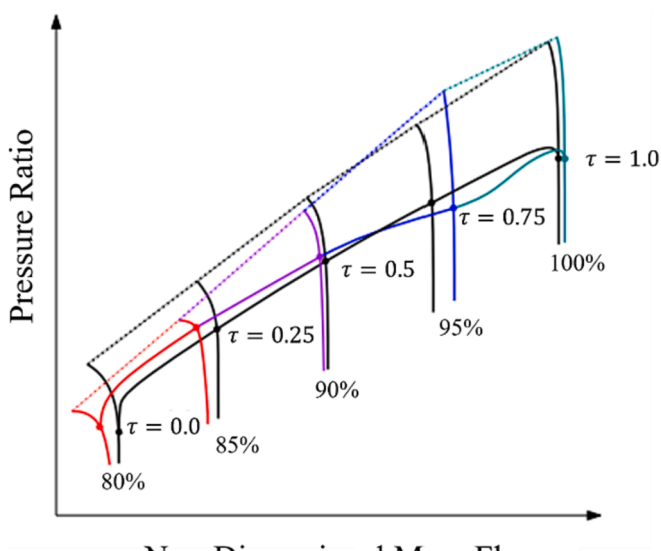


Fig. 16. Example schematic diagram of a composite compressor map used to represent the unsteady properties of velocity and stall lines during transient with heat transfer [160].

5. The research current status, challenges and future for transient simulation analysis

This paper provides a comprehensive review of the simulation of transients and heat transfer effects related to gas turbine engines. Over the past 70 years, significant progress has been made in improving the accuracy, fidelity, and speed of transient and heat transfer effect simulations. The article includes a detailed discussion of the development of methodologies and their application to gas turbine transient simulation, as well as the impact of heat transfer on transient performance. Through critical analysis, a comprehensive supporting document for future gas turbine transient and heat transfer effect simulation has been created. However, challenges still exist, and certain aspects require further consideration. This section will discuss the remaining challenges and potential future development in gas turbine engine transient simulation and heat transfer effect modelling.

5.1. Transient performance simulation

The challenges and possible solutions related to the transient simulation can be concluded in the next few points:

1. Current white box approach lacks the capability of capturing several thermal dynamic phenomena.

As concluded by Table 1, it is clear that different white box transient simulation methodologies have their shortage. The CMF method can offer a more accurate outcome. However, it neglects the volume dynamic effect. For the ICV method, it considers the volume dynamic, but it has the map reading problem and the selection of time step need to be careful. For PWV, it includes the pressure wave phenomena but that extends the calculation time significantly. For the IMF method, it solves the map reading problem but leads to relatively lower accuracy. Therefore, an improved transient simulation methodology is probably still attainable. A method with the capability of capturing several dynamic effects without losing accuracy and calculation speed is recommended. However, a detailed method cannot be raised now.

2. Current black box training data lacks the consideration of the heat transfer effect.

The black box approach is getting increased attention nowadays. More research has been focused on the use of the black box approach for gas turbine transient simulation, and promising outcomes have been produced. However, it is found that the training data for the black box models are usually the simulation outcome without considering the secondary effect coming from heat soakage, tip clearance moving and component characteristic change. To move one step ahead, researchers can consider these effects when they build and train the black box model.

3. Current CFD simulation lacks the consideration of full-size gas turbine transient simulation.

CFD plays an important role in gas turbine design. In the transient field, attention has been made to the component transient performance simulation [67,68]. However, due to the extremely high computational cost and demand of geometry information, only a limited number of research is found related to the gas turbine overall transient simulation [77,78,79]. Since CFD is suitable for 2D and 3D flow field simulations, it has the potential to reveal a more accurate gas turbine transient performance. So, the development of full-size gas turbine transient CFD models is recommended.

Table 3

Comparison between different component characteristic modification methodologies.

Author	Basic Idea	Advantage	Disadvantage
Pilidis and Maccallum (1986) [147,153]	Obtaining new shaft rotational speed and surge margin based on the empirical correlation	• Easy to be implemented	• Only suitable for certain compressor • High cost of modelling
Torella (1990) [157]	Obtaining a new component efficiency based on the empirical correlation.	• Easy to be implemented	• Without considering the flow dynamic change
Kiss and Spakovszky (2015) [160,161]	Using composite compressor map that includes heat transfer effect for a certain transient process.	• High accuracy • Direct use of map instead of modifying during transient	• Only suitable for certain transient process • Heat flow estimation based on adiabatic condition
Li (2019) [162]	Using scaling factor to modify the map at each time interval.	• Considering the time-dependent heat transfer effect on the map	• Low accuracy due to direct use of index value from Pilidis and Maccallum's work when the type of gas turbine was different

5.2. Heat transfer effect on transient performance

The challenges and possible solutions related to the heat transfer effect simulation can be concluded in the next points:

1. Current heat transfer effect analysis lacks the consideration of tip and axial clearance change coming from the axial movement of components.

The component axial movements will affect the tip clearance [59]. Also, the component thermal displacement will affect the blade axial clearance. However, most of the critical investigations, such as MacCallum and Pilidis's work, Khalid and Hearne's work and Li's work, neglect the horizontal expansion and contraction of blade casing and disc [38,62,80]. Several studies had reported that the variation of the temperature field in the compressor leads to the different thermal expansion of the casing and rotor, which leads to the deviation of the axial clearance between the rotor and rotor blades from the design point, thus affecting the performance of the compressor [163,164]. For a more accurate simulation of the heat transfer effect, an axial clearance model is recommended during the investigation.

2. Current heat transfer effect analysis lacks the consideration of a detailed combustor heat transfer model.

During the combustor heat soakage analysis, it was always estimated based on the mean temperature of inlet and outlet conditions or was even neglected during the heat transfer effect analysis [40,109,111,114,117,118,127,128,162]. However, the temperature distribution along the combustor is non-linear due to the different combustion processes in the primary, secondary, and dilution zones. A proper model should be established for a more realistic combustor heat soakage calculation. A heat transfer model based on 1-D or 2-D that can capture temperature distribution along the combustor, the radiative heat transfer, TBC and the film cooling, and secondary air flow is suggested for the combustor when investigating the combustor heat soakage effect.

3. Creating an advanced component map for individual engine components.

Compared to the attention given to the heat soakage and tip clearance effects, the modification of component characteristic maps has received relatively little consideration. Only two novel methodologies have been proposed in the past 20 years. Naylor has highlighted that the most accurate, easiest, and quickest method for calculation is the component map look-up approach [40]. Current component performance maps are typically based on adiabatic conditions. One potential solution is to create diabatic component maps that include the heat soakage and tip clearance movement effects and use them during transient simulations. Kiss's method follows this idea, but each composite

map can only be applied to a specific transient process. However, to capture the effects of heat soakage on the whole engine performance in a variety of transient operating conditions, advanced component maps should be implemented. These maps should contain diabatic information on the relationship between heat flux, tip clearance, rotational speed, and mass flow for engine components. Based on the advanced component map, extremely fast and accurate results under different gas turbine transient conditions can be obtained. Hence, it provides a potential future research horizon.

6. Conclusion

This paper aims to critically analyze the aspects of gas turbine transient simulation. A comprehensive review of the methodology development and application of gas turbine transient simulation and heat transfer effect simulation has been presented, covering its development since the 1950 s up to current state-of-the-art practices. Moreover, the development of transient simulation platforms has been included because it assisted engineers and gas turbine operators during the gas turbine design phase.

Fast and accurate simulation is always needed for the gas turbine transient simulation. The white box approach plays an important role in the development of transient simulation. Features such as shaft dynamic, volume dynamic, and pressure wave effect are continuously investigated and added to the simulation to make it more accurate. Both static and dynamic NN approaches are discussed for the black box approach. The black box approach starts getting more attention because it can offer a relatively reliable outcome with a fast calculation speed when specific gas turbine data are missing. Besides, the numerical approach (CFD) is discussed due to its specific role in transient simulation development. Based on the in-depth discussion, challenges and possible solutions have been raised. A more accurate method that can capture several dynamic effects without losing accuracy and calculation speed is recommended for the white box approach, while black box building and training processes are suggested to include the heat transfer effects. For the CFD approach, the development of full-size gas turbine transient models is recommended.

For the heat transfer effect, it is identified due to the mismatch between the gas turbine transient simulation outcome and the experiment data. Three main parts are included: heat soakage effect, tip clearance effect and component characteristic change effect. These effects are negligible during the gas turbine steady state. However, during the transient, the large heat flow between the engine metal and the working gas will lead to a large heat transfer and, in addition, affect the component and whole engine performance. For heat soakage effect and tip clearance, efforts have been made to the establishment of more realistic heat transfer models. For component characteristics change effect, efforts have been made to the establishment of non-adiabatic component performance maps. Challenges and potential solutions have also been raised. The axial clearance movement and combustor axial temperature distribution are suggested to be considered for a more

accurate heat transfer estimation. The creation of an advanced component map is recommended since it will be accurate and fast.

Declaration of Competing Interest

The authors declare that they have no known competing financial interests or personal relationships that could have appeared to influence the work reported in this paper.

Data availability

No data was used for the research described in the article.

References

- [1] P.P. Walsh, P. Fletcher, *Gas Turbine Performance*, second ed., Oxford Blackwell Science, 2004.
- [2] H.I.H. Saravanamuttoo, G.F.C. Rogers, H. Cohen, *Gas Turbine Theory*, Sixth ed., Pearson Prentice Hall, 2009.
- [3] M. Darecki et al., Flightpath 2050 Europe's vision for aviation : maintaining global leadership and serving society's needs, 2011. <https://op.europa.eu/en/publication-detail/-/publication/296a9bd7-fe9f-4ae8-82c4-a21ff48be673> (accessed 14 March 2023).
- [4] A.J. Fawke, H.I.H. Saravanamuttoo, Digital Computer Methods for Prediction of Gas Turbine Dynamic Response, Feb. 1971, 10.4271/710550.
- [5] J. SZUCHI, Advancements in real-time engine simulation technology, Jun. 1982, 10.2514/6.1982-1075.
- [6] C. Evans, Testing and modelling aircraft gas turbines: an introduction and overview, in: UKACC International Conference on Control (CONTROL '98), 1998, vol. 1998, no. 455, pp. 1361–1366, 10.1049/cp:19980428.
- [7] V. Sanghi, B.K. Lakshmanan, V. Sundararajan, Survey of advancements in jet-engine thermodynamic simulation, *J. Propul. Power* 16 (5) (Sep. 2000) 797–807, <https://doi.org/10.2514/2.5644>.
- [8] M.B. Hashmi, T.A. Lemma, S. Ahsan, S. Rahman, Transient behavior in variable geometry industrial gas turbines: a comprehensive overview of pertinent modeling techniques, *Entropy* 23 (2) (Feb. 2021) 250, <https://doi.org/10.3390/e23020250>.
- [9] H. Asgari, X. Chen, M.B. Menhaj, R. Sainudiin, Artificial neural network-based system identification for a single-shaft gas turbine, *J. Eng. Gas Turbines Power* 135 (9) (Sep. 2013), <https://doi.org/10.1115/1.4024735>.
- [10] N.R.L. MacCallum, The Performance of turbojet engines during the 'Thermal Soak' transient, *Proc. Inst. Mech. Eng. Conf. Proc.* 184 (7) (Sep. 1969) 23–29, https://doi.org/10.1243/PIME_CONF_1969_184_179_02.
- [11] M. Jelali, A. Kroll, *Hydraulic Servo-systems: Modelling, Identification, and Control*, first ed., Springer, 2003.
- [12] L.L. Jaw, S. Garg, Propulsion control technology development in the United States A historical perspective, NASA Technical Memorandum, NASA/TM-2005-213978, 2005.
- [13] E.W. Otto, I. Burt, L. Taylor, Dynamics of a turbojet engine considered as a quasi-static system, NACA Technical Notes 2091, 1950.
- [14] H. Gold, S. Rosenzweig, *A method for estimating speed response of gas-turbine engines*, NACA Res. Memor. E51K21 (1952).
- [15] J.O.N. Lawrence, R.D. Powell, The application of servo-mechanism analysis to fuel control problems, *Proc. Inst. Mech. Eng.* 172 (1) (Jun. 1958) 439–469, https://doi.org/10.1243/PIME_PROC_1958_172_039_02.
- [16] D. Novik, Some linear dynamics of two-spool turbojet engines, NACA Technical Notes 3274 (1956).
- [17] J.F. Dugan, Component operating trends during acceleration and deceleration of two hypothetical two spool engines, NACA Res. Memor. E54L28 (1955).
- [18] R.E. Filippi, J.F. Dugan, Effect of design over all compressor pressure ratio division on acceleration characteristics of three hypothetical two-spool turbojet engines, NACA Res. Memor. E56D13 (1956).
- [19] V.L. Larrove, M.M. Spencer, M. Tribus, A dynamic performance computer for gas-turbine engines, *J. Fluids Eng.* 79 (7) (Oct. 1957) 1707–1714, <https://doi.org/10.1115/1.4013457>.
- [20] C. Kong, J. Ki, K. Koh, Steady-state and transient performance simulation of a turboshaft engine with free power turbine, in: Volume 2: Coal, Biomass and Alternative Fuels; Combustion and Fuels; Oil and Gas Applications; Cycle Innovations, Jun. 1999, vol. 2, 10.1115/99-GT-375.
- [21] W.J. Tong, S.J. Tang, Geared turbofan engine transient modeling research based on CMF method, *Hangkong Dongli Xuebao/J. Aerosp. Power* 26 (6) (2011) 1377–1383, <https://doi.org/10.13224/j.cnki.jasp.2011.06.029>.
- [22] G. Wortmann, O. Schmitz, M. Hormung, Comparative assessment of transient characteristics of conventional and hybrid gas turbine engine, *CEAS Aeronaut. J.* 5 (2) (Jun. 2014) 209–223, <https://doi.org/10.1007/s13272-014-0101-8>.
- [23] M. Montero Carrero, M.L. Ferrari, W. De Paepe, A. Parente, S. Bram, F. Contino, Transient Simulations of a T100 Micro Gas Turbine Converted Into a Micro Humid Air Turbine, in: Volume 3: Coal, Biomass and Alternative Fuels; Cycle Innovations; Electric Power; Industrial and Cogeneration, Jun. 2015, vol. 3, pp. 1–9, 10.1115/GT2015-43277.
- [24] M. Raggio, D. Bellotti, M.L. Ferrari, Transient Analysis of a Micro Gas Turbine With Fuel Composition Change, in: Volume 4: Cycle Innovations; Cycle Innovations: Energy Storage, Jun. 2022, vol. 4, pp. 1–10, 10.1115/GT2022-81300.
- [25] M.J. Kim, J.H. Kim, T.S. Kim, Program development and simulation of dynamic operation of micro gas turbines, *Appl. Therm. Eng.* 108 (2016) 122–130, <https://doi.org/10.1016/j.applthermaleng.2016.07.103>.
- [26] F. Mueller, R. Gaynor, A.E. Auld, J. Brouwer, F. Jabbari, G.S. Samuels, Synergistic integration of a gas turbine and solid oxide fuel cell for improved transient capability, *J. Power Sources* 176 (1) (Jan. 2008) 229–239, <https://doi.org/10.1016/j.jpowsour.2007.10.081>.
- [27] V. Singh, L.-U. Axelsson, W.P.J. Visser, Transient Performance Analysis of an Industrial Gas Turbine Operating on Low-Calorific Fuels, in: Volume 8: Microturbines, Turbochargers and Small Turbomachines; Steam Turbines, Jun. 2016, vol. 8, pp. 1–9, 10.1115/GT2016-57523.
- [28] A.J. Fawke, H.I.H. Saravanamuttoo, Experimental investigation of methods for improving the dynamic response of a twin-spool turbojet engine, *J. Eng. Power* 93 (4) (Oct. 1971) 418–424, <https://doi.org/10.1115/1.3445601>.
- [29] L. Chuankai, Q. Tian, D. Shuiting, Transient analysis of volume packing effects on turbofan engine, *Procedia Eng.* 17 (2011) 549–558, <https://doi.org/10.1016/j.proeng.2011.10.068>.
- [30] K. Chung, K. Leamy, T. Collins, A Turbine Engine Aerodynamic Model for In-stall Transient Simulation, Jul. 1985, 10.2514/6.1985-1429.
- [31] T. Haykin, S. Murthy, Transient engine performance with water ingestion, in: 22nd Joint Propulsion Conference, Jun. 1986, vol. 4, no. 1, 10.2514/6.1986-1621.
- [32] R. Yadav, Y. Kapadi, A. Pashikar, Aero-Thermodynamic Model for Digital Simulation of Turbofan Engine, in: Volume 1: Turbo Expo 2005, Jan. 2005, vol. 1, no. January, pp. 63–70, 10.1115/GT2005-68248.
- [33] A. Traverso, F. Calzolari, A. Massardo, Transient Analysis of and Control System for Advanced Cycles Based on Micro Gas Turbine Technology, in: Volume 3: Turbo Expo 2003, Jan. 2003, vol. 3, no. June 2003, pp. 201–209, 10.1115/GT2003-38269.
- [34] A. Traverso, R. Scarpellini, A. Massardo, Experimental Results and Transient Model Validation of an Externally Fired Micro Gas Turbine, in: Volume 5: Turbo Expo 2005, Jan. 2005, vol. 5, pp. 35–43, 10.1115/GT2005-68100.
- [35] C. Wang, Y.G. Li, B.Y. Yang, Transient performance simulation of aircraft engine integrated with fuel and control systems, *Appl. Therm. Eng.* 114 (Mar. 2017) 1029–1037, <https://doi.org/10.1016/j.applthermaleng.2016.12.036>.
- [36] S. Shamekhii Amiri, J. Al-Zaili, A.I. Sayma, Development of a Dynamic Model for Simulating the Transient Behaviour of a Solar-Powered Micro Gas Turbine, in: Volume 4: Cycle Innovations; Cycle Innovations: Energy Storage, Jun. 2022, vol. 4, pp. 1–10, 10.1115/GT2022-79059.
- [37] A.J. Fawke, H.I.H. Saravanamuttoo, M. Holmes, Experimental verification of a digital computer simulation method for predicting gas turbine dynamic behaviour, *Proc. Inst. Mech. Eng.* 186 (1) (Jun. 1972) 323–329, https://doi.org/10.1243/PIME_PROC_1972_186_035_02.
- [38] A. Nishi, T. Sawada, Digital simulation of a variable geometry gas turbine, *Bull. Univ. Osaka Prefect. Ser. A, Eng. Nat. Sci.*, 23, no. 2, pp. 111–125, 1974, 10.24729/00008728.
- [39] P. Pilidis, *Digital Simulation of Gas Turbine Performance*, University of Glasgow, 1983. Ph.D. thesis.
- [40] P.H. Naylor, *Gas Turbine Transient Performance: Heat Soakage Modelling*, Cranfield University, 2004. Ph.D thesis.
- [41] N.U. Rahman, J.F. Whidborne, Real-time transient three spool turbofan engine simulation: a hybrid approach, *J. Eng. Gas Turbines Power* 131 (5) (Sep. 2009) 1–8, <https://doi.org/10.1115/1.3079611>.
- [42] Y.G. Li, N.R.L. MacCallum, P. Pilidis, Pressure waves in volume effect in gas-turbine transient-performance models, *J. Propul. Power* 17 (3) (May 2001) 706–710, <https://doi.org/10.2514/2.5799>.
- [43] E. Tsoutsanis, N. Meskin, M. Benamar, K. Khorasani, Dynamic performance simulation of an aeroderivative gas turbine using the matlab simulink environment, *ASME Int. Mech. Eng. Congr. Expo. Proc.* 4 A (2013) 1–10, <https://doi.org/10.1115/IMECE2013-64102>.
- [44] Z. Li, *Aircraft Engine Transient Performance Modelling with Heat Soakage effects*, Cranfield University, 2019. Ph.D thesis.
- [45] H. Asgari, X. Chen, *Gas Turbines Modeling, Simulation, and Control*, First ed., CRC Press, 2015.
- [46] H. Asgari et al., Modeling and Simulation of the Start-Up Operation of a Heavy-Duty Gas Turbine by Using NARX Models, in: Volume 3A: Coal, Biomass and Alternative Fuels; Cycle Innovations; Electric Power; Industrial and Cogeneration, Jun. 2014, pp. 1–10, 10.1115/GT2014-25056.
- [47] N. Chiras, C. Evans, D. Rees, Global nonlinear modeling of gas turbine dynamics using NARMAX structures, *J. Eng. Gas Turbines Power* 124 (4) (Oct. 2002) 817–826, <https://doi.org/10.1115/1.1470483>.
- [48] A.E. Ruano, P.J. Fleming, C. Teixeira, K. Rodriguez-Vázquez, C.M. Fonseca, Nonlinear identification of aircraft gas-turbine dynamics, *Neurocomputing* 55 (3–4) (Oct. 2003) 551–579, [https://doi.org/10.1016/S0925-2312\(03\)00393-X](https://doi.org/10.1016/S0925-2312(03)00393-X).
- [49] A. Gambarotta, I. Vaja, A real time dynamic model of a micro - Gas turbine CHP system with regeneration, *Proc. ASME Power Conf.* 2007 (2007) 575–586, <https://doi.org/10.1115/POWER2007-22098>.
- [50] R. Rezvani et al., A Gas Turbine Engine Model of Transient Operation Across the Flight Envelope, in: Volume 3: Controls, Diagnostics and Instrumentation; Education; Electric Power; Microturbines and Small Turbomachinery; Solar Brayton and Rankine Cycle, Jan. 2011, vol. 3, pp. 133–140, 10.1115/GT2011-45565.

- [51] M. Rahnama, H. Ghorbani, A. Montazeri, Nonlinear identification of a gas turbine system in transient operation mode using neural network, in: 4th Conference on Thermal Power Plants, 2012, pp. 1–6.
- [52] R. Khalili, M. Karrari, Modeling and identification of an industrial gas turbine using classical and non-classical approaches, in: 2017 Iranian Conference on Electrical Engineering (ICEE), May 2017, no. Ieee2017, pp. 667–672, 10.1109/IranianCEE.2017.7985123.
- [53] I. Koleini, A. Roudbari, V. Marefat, EGT prediction of a micro gas turbine using statistical and artificial intelligence approach, *IEEE Aerosp. Electron. Syst. Mag.* 33 (7) (2018) 4–13, <https://doi.org/10.1109/MAES.2018.170045>.
- [54] S. Kim, K. Kim, C. Son, Transient system simulation for an aircraft engine using a data-driven model, *Energy* 196 (Apr. 2020), 117046, <https://doi.org/10.1016/j.energy.2020.117046>.
- [55] B. Wu, Dynamic performance simulation analysis method of split shaft gas turbine based on RBF neural network, *Energy Rep.* 7 (Nov. 2021) 947–958, <https://doi.org/10.1016/j.egyr.2021.09.178>.
- [56] I. Ibrahim, O. Akhrif, H. Moustapha, M. Staniszewski, Neural Networks Modelling of Aero-derivative Gas Turbine Engine: A Comparison Study, in: Proceedings of the 16th International Conference on Informatics in Control, Automation and Robotics, 2019, vol. 1, no. Icinco, pp. 738–745, 10.5220/0007928907380745.
- [57] I.M.A. Ibrahim, O. Akhrif, H. Moustapha, M. Staniszewski, An ensemble of recurrent neural networks for real time performance modeling of three-spool aero-derivative gas turbine engine, *J. Eng. Gas Turbines Power* 143 (10) (Oct. 2021) 1–10, <https://doi.org/10.1115/1.4051112>.
- [58] H. Asgari, M. Venturini, X. Chen, R. Sainudiin, Modeling and simulation of the transient behavior of an industrial power plant gas turbine, *J. Eng. Gas Turbines Power* 136 (6) (Jun. 2014) 1–10, <https://doi.org/10.1115/1.4026215>.
- [59] F. Jurado, Non-linear modeling of micro-turbines using NARX structures on the distribution feeder, *Energy Convers. Manag.* 46 (3) (Feb. 2005) 385–401, <https://doi.org/10.1016/j.enconman.2004.03.012>.
- [60] H. Asgari, et al., NARX models for simulation of the start-up operation of a single-shaft gas turbine, *Appl. Therm. Eng.* 93 (Jan. 2016) 368–376, <https://doi.org/10.1016/j.applthermeng.2015.09.074>.
- [61] H. Asgari, E. Ory, Prediction of Dynamic Behavior of a Single Shaft Gas Turbine Using NARX Models, in: Volume 6: Ceramics and Ceramic Composites; Coal, Biomass, Hydrogen, and Alternative Fuels; Microturbines, Turbochargers, and Small Turbomachines, Jun. 2021, vol. 6, pp. 1–10, 10.1115/GT2021-58960.
- [62] B. Yu, W. Shu, Research on turbofan engine model above idle state based on NARX modeling approach, *IOP Conf. Ser. Mater. Sci. Eng.* 187 (1) (Mar. 2017), 012002, <https://doi.org/10.1088/1757-899X/187/1/012002>.
- [63] H. Bahlawani, M. Morini, M. Pinelli, P. Ruggero Spina, M. Venturini, Development of reliable NARX models of gas turbine cold, warm, and hot start-up, *J. Eng. Gas Turbines Power* 140 (7) (Jul. 2018), <https://doi.org/10.1115/1.4038838>.
- [64] E. Ory, H. Asgari, Machine learning approaches for modelling a single shaft gas turbine, *Int. J. Model. Ident. Control* 37 (3/4) (2021) 275, <https://doi.org/10.1504/IJMIC.2021.10045910>.
- [65] M. Alsarayreh, O. Mohamed, M. Matar, Modeling a practical dual-fuel gas turbine power generation system using dynamic neural network and deep learning, *Sustainability* 14 (2) (Jan. 2022) 870, <https://doi.org/10.3390/su14020870>.
- [66] S. Murari, S. Sunnam, J.S. Liu, Steady state and transient CFD studies on aerodynamic performance validation of a high pressure turbine, in: Volume 8: Turbomachinery, Parts A, B, and C, Jun. 2012, pp. 2067–2077, 10.1115/GT2012-68853.
- [67] J.D. Denton, W.N. Dawes, Computational fluid dynamics for turbomachinery design, *Proc. Inst. Mech. Eng. Part C J. Mech. Eng. Sci.* 213 (2) (Feb. 1998) 107–124, <https://doi.org/10.1243/0954406991522211>.
- [68] J. Tyacke, N.R. Vadlamani, W. Trojak, R. Watson, Y. Ma, P.G. Tucker, Turbomachinery simulation challenges and the future, *Prog. Aerosp. Sci.* 110 (April) (Oct. 2019), 100554, <https://doi.org/10.1016/j.paerosci.2019.100554>.
- [69] R. Blumenthal, B. Hutchinson, L. Zori, Investigation of Transient CFD Methods Applied to a Transonic Compressor Stage, in: Volume 7: Turbomachinery, Parts A, B, and C, Jan. 2011, vol. 7, no. PARTS A, B, AND C, pp. 1423–1430, 10.1115/GT2011-46635.
- [70] M.A. Qizar, M.L. Mansour, S. Goswami, Study of steady state and transient blade row CFD methods in a moderately loaded NASA transonic high-speed axial compressor stage, in: Volume 6B: Turbomachinery, Jun. 2013, vol. 6 B, pp. 1–9, 10.1115/GT2013-94739.
- [71] H. Roclawski, M. Gugau, M. Böhle, Computational fluid dynamics analysis of a radial turbine during load step operation of an automotive turbocharger, *J. Fluids Eng.* 140 (2) (Feb. 2018) 1–9, <https://doi.org/10.1115/1.4037975>.
- [72] C. Cornelius, T. Biesinger, P. Galpin, A. Braune, Experimental and computational analysis of a multistage axial compressor including stall prediction by steady and transient CFD methods, *J. Turbomach.* 136 (6) (2014) 1–12, <https://doi.org/10.1115/1.4025538>.
- [73] D. Kim, S. Kim, C. Son, K. Kim, M. Kim, S. Min, Transient performance prediction of an axial compressor considering VIGV operation speeds, *J. Mech. Sci. Technol.* 28 (10) (2014) 4099–4107, <https://doi.org/10.1007/s12206-014-0923-7>.
- [74] P.K. Mohammadian, M.H. Saidi, Simulation of startup operation of an industrial twin-shaft gas turbine based on geometry and control logic, *Energy* 183 (Sep. 2019) 1295–1313, <https://doi.org/10.1016/j.energy.2019.07.030>.
- [75] J.S. Litt, Y. Liu, T.S. Sowers, A.K. Owen, T.-H. Guo, Validation of an Integrated Airframe and Turbofan Engine Simulation for Evaluation of Propulsion Control Modes, in: 53rd AIAA Aerospace Sciences Meeting, Jan. 2015, no. January, pp. 1–18, 10.2514/6.2015-1476.
- [76] H. Chang, W. Zhao, D. Jin, Z. Peng, X. Gui, Numerical investigation of base-setting of stator's stagger angles for a 15-stage axial-flow compressor, *J. Therm. Sci.* 23 (1) (2014) 36–44, <https://doi.org/10.1007/s11630-014-0674-x>.
- [77] R. Marsilio, A Computational Method For Gas Turbine Engines, in: 43rd AIAA Aerospace Sciences Meeting and Exhibit, Jan. 2005, no. January, pp. 49–57, 10.2514/6.2005-1009.
- [78] M. Ferlauto, R. Marsilio, Simulation of Jet Engine Transients by a CFD Method, in: 42nd AIAA/ASME/SAE/ASEE Joint Propulsion Conference & Exhibit, Jul. 2006, no. July, 10.2514/6.2006-4968.
- [79] M. Ferlauto, R. Marsilio, Numerical simulation of the unsteady flowfield in complete propulsion systems, *Adv. Aircr. Spacecr. Sci.* 5 (3) (2018) 349–362, <https://doi.org/10.12989/aas.2018.5.3.349>.
- [80] W.G. Joo, T.P. Hynes, The simulation of turbomachinery blade rows in asymmetric flow using actuator disks, *J. Turbomach.* 119 (4) (Oct. 1997) 723–732, <https://doi.org/10.1115/1.2841182>.
- [81] J. Göing, A. Kellersmann, C. Bode, J. Friedrichs, Jet Propulsion Engine Modelling Using Pseudo Bond Graph Approach, in: Volume 1: Aircraft Engine; Fans and Blowers; Marine; Honors and Awards, Jun. 2019, vol. 1, pp. 1–11, 10.1115/GT2019-90420.
- [82] J. Göing, S. Lück, C. Bode, J. Friedrichs, Performance Simulation to Investigate the Impact of a Deteriorated High-Pressure Compressor on Turbofan Engine Using a Pseudo Bond Graph Modelling Approach, Sep. 2019, pp. 4–11, 10.33737/gppsp19-bj-160.
- [83] B.D. MacIsaac, H.I.H. Saravanamuttoo, A Comparison of Analog, Digital and Hybrid Computing Techniques for Simulation of Gas Turbine Performance, in: Volume 1B: General, Mar. 1974, vol. 1B: Genera, 10.1115/74-GT-127.
- [84] J. Sellers, C. Daniele, Dyneng - a Program and for Calculating Performance of Turbojet Transient, NASA Technical Note, NASA-TN-D-7901, 1975.
- [85] C.J. Daniele, S.M. Krosl, R. Szuch, E.J. Westerkamp, Digital Computerprogram for Generating Dynamical Turbofan Engine Models (Digitem), NASA/TM-83446, 1983. NASA Tech. Memo.
- [86] G. Sadler, K. Melcher, DEAN - a program for Dynamic Engine ANalysis, Jul. 1985, 10.2514/6.1985-1354.
- [87] J.R. Szuch, HYDECS: A generalized hybrid computer program for studying turbojet or turbofan engine dynamics, NASA Technical Memorandum, NASA-TM-X-3014, 1974.
- [88] R.W. Koenig, L.H. Fisbbacb, GENENG—A Program for Calculating Design and Off-Design Performance for Turbojet and Turbofan Engines, NASA Technical Note, NASA-TN-D-6552, 1972.
- [89] T. Schobeiri, M. Abouelkheir, C. Lippke, Getran: A geimeraic, modularly structured computer code for simulation of dynamic behavior of aero- and power generation gas turbine engines, in: ASME 1993 Int. Gas Turbine Aeroengine Congr. Expo. GT 1993, vol. 3C, no. 93, 1993 10.1115/93-GT-388.
- [90] J.A. Reed, A.A. Afjeh, Computational Simulation of Gas Turbines: Part I — Foundations of Component-Based Models, in: Volume 1: Aircraft Engine; Marine; Turbomachinery; Microturbines and Small Turbomachinery, Jun. 1999, vol. 1, 10.1115/99-GT-346.
- [91] J.A. Reed, A.A. Afjeh, Computational Simulation of Gas Turbines: Part II — Extensible Domain Framework, in: Volume 1: Aircraft Engine; Marine; Turbomachinery; Microturbines and Small Turbomachinery, Jun. 1999, vol. 1, 10.1115/99-GT-347.
- [92] J.K. Lytle, The Numerical Propulsion System Simulation: A Multidisciplinary Design System for Aerospace Vehicles, Nasa Technical Memorandum, NASA/TM-1999-20194, 1999.
- [93] J.K. Lytle, The Numerical Propulsion System Simulation: An Overview, NASA Technical Report, 2000. <https://ntrs.nasa.gov/citations/20000063377>.
- [94] C. Argote, B.K. Kestner, D.N. Mavris, NPSS volume dynamic capability for real-time physics based engine modeling, Proc. ASME Turbo Expo 1 (2011) 139–148, <https://doi.org/10.1115/GT2011-45374>.
- [95] D.E. Hirst, Digital simulation of nonlinear dynamic systems using standard FORTRAN, *Electron. Lett.* 7 (4) (1971) 102, <https://doi.org/10.1049/el:19710069>.
- [96] J.R. Palmer, Y. Cheng-Zhong, Turboparts — a programming language for the performance simulation of arbitrary gas turbine engines with arbitrary control systems, *Int. J. Turbo Jet Engines* 2 (1) (Jan. 1985) 1–8, <https://doi.org/10.1515/TJJ.1985.2.1.19>.
- [97] A. Traverso, TRANSEO code for the dynamic performance simulation of micro gas turbine cycles, *Proc. ASME Turbo Expo* 5 (2005) 45–54, <https://doi.org/10.1115/GT2005-68101>.
- [98] M.A. Chappell, E.G. Blevins, Advanced turbine engine simulation technique development and applications to testing, *AIAA Pap.* (1986), <https://doi.org/10.2514/6.1986-1731>.
- [99] M. Chappell, P. McLaughlin, An approach to modeling continuous turbine engine operation from startup to shutdown, in: 27th Joint Propulsion Conference, Jun. 1991, vol. 9, no. 3, 10.2514/6.1991-2373.
- [100] J. Kurzke, Advanced User-Friendly Gas Turbine Performance Calculations on a Personal Computer, in: Volume 5: Manufacturing Materials and Metallurgy; Ceramics; Structures and Dynamics; Controls, Diagnostics and Instrumentation; Education; IGTI Scholar Award, Jun. 1995, vol. 5, 10.1115/95-GT-147.
- [101] W.P.J. Visser, M.J. Broomhead, GSP, a Generic Object-Oriented Gas Turbine Simulation Environment, in: Volume 1: Aircraft Engine; Marine; Turbomachinery; Microturbines and Small Turbomachinery, May 2000, vol. 1, no. May 2000, pp. 1–8, 10.1115/2000-GT-0002.
- [102] A. Alexiou, K. Mathioudakis, Development of Gas Turbine Performance Models Using a Generic Simulation Tool, in: Volume 1: Turbo Expo 2005, Jan. 2005, pp. 185–194, 10.1115/GT2005-68678.

- [103] A. Bala, V. Sethi, E.L.E. Lo Gatto, V. Pachidis, P. Pilidis, PROOSIS—A Collaborative Venture for Gas Turbine Performance Simulation using an Object Oriented Programming Schema,” no. July, 2007, https://www.researchgate.net/publication/253000147_PROOSIS_-A_Collaborative_Venture_for_Gas_Turbine_Performance_Simulation_using_an_Object_Oriented_Programming_Schema (accessed 13 May 2023).
- [104] <https://www.plm.automation.siemens.com/global/en/products/simulation-test/propulsion-system-simulation.html> (access on 15-11-2022).
- [105] I. Roumeliotis, T. Nikolaidis, V. Pachidis, O. Broca, D. Unlu, Dynamic Simulation of a Rotorcraft Hybrid Engine in Simcenter Amesim, in: 44th European Rotorcraft Forum, 2018, pp. 37–39.
- [106] C. Daguang, P. Yongquan, Thermal effects on transient process of a turbojet engine, *Hangkong Dongli Xuebao/J. Aerosp. Power* 2 (1) (1987) 85–86.
- [107] K. Bauerfeind, Die exakte Bestimmung des Uebertragungsverhaltens von Turbostrahltriebwerken unter Berücksichtigung des instationären Verhaltens seiner Komponenten, PhD thesis in German, Fakultät für Maschinenwesen und Elektrotechnik der Technischen Hochschule Muench, 1968.
- [108] A.J. Fawke, H.I.H. Saravananutto, Digital computer simulation of the dynamic response of a twin-spool turbofan with mixed exhausts, *Aeronaut. J.* 77 (753) (1973) 471–478, <https://doi.org/10.1017/S0001924000041567>.
- [109] S. Khalid, R. Hearne, Enhancing dynamic model fidelity for improved prediction of turbofanengine transient performance, Jun. 1980, 10.2514/6.1980-1083.
- [110] S. Kim, K. Kim, C. Son, A new transient performance adaptation method for an aero gas turbine engine, *Energy* 193 (2020), 116752, <https://doi.org/10.1016/j.energy.2019.116752>.
- [111] W.P.J. Visser, I.D. Dountchev, Modeling Thermal Effects on Performance of Small Gas Turbines, in: Volume 1: Aircraft Engine; Fans and Blowers; Marine, Jun. 2015, vol. 1, pp. 1–12. 10.1115/GT2015-42744.
- [112] J.W. Chapman, T.-H. Guo, J.L. Kratz, J.S. Litt, Integrated Turbine Tip Clearance and Gas Turbine Engine Simulation, in: 52nd AIAA/SAE/ASEE Joint Propulsion Conference, Jul. 2016, pp. 1–16, 10.2514/6.2016-5047.
- [113] J.L. Kratz, D.E. Culley, J.W. Chapman, Approximation of Engine Casing Temperature Constraints for Casing Mounted Electronics, in: 52nd AIAA/SAE/ASEE Joint Propulsion Conference, Jul. 2016, pp. 1–23, 10.2514/6.2016-4858.
- [114] F. Chen, Y. Chen, K. Song, Y. Li, Study on the Influence of Heat Transfer Effect on Performance Simulation of Engine Transition State, in: 2019 IEEE 10th International Conference on Mechanical and Aerospace Engineering (ICMAE), Jul. 2019, pp. 443–448, 10.1109/ICMAE.2019.8880972.
- [115] R.S. Merkler, S. Staudacher, Modeling of Heat Transfer and Clearance Changes in Transient Performance Calculations: A Comparison, in: Volume 2: Aircraft Engine; Ceramics; Coal, Biomass and Alternative Fuels; Controls, Diagnostics and Instrumentation; Environmental and Regulatory Affairs, Jan. 2006, pp. 37–45, 10.1115/GT2006-90041.
- [116] C. Riegler, Correlations to include heat transfer in gas turbine performance calculations, *Aerosp. Sci. Technol.* 3 (5) (Jul. 1999) 281–292, [https://doi.org/10.1016/S1270-9638\(00\)86964-3](https://doi.org/10.1016/S1270-9638(00)86964-3).
- [117] M. Vieweg, F. Wolters, R.-G. Becker, Comparison of a Heat Soakage Model With Turbofan Transient Engine Data, in: Volume 1: Aircraft Engine; Fans and Blowers; Marine; Honors and Awards, Jun. 2017, vol. 1, pp. 1–12. 10.1115/GT2017-63461.
- [118] T. Qiuyue, J. Rui, X. Xuan, Z. Heng, Y. Hongming, Effects of heat soakage on transient performance of gas turbine engine, *J. Aerosp. Power* 32(3) (2017) 630–636, 10.13224/j.cnki.jasp.2017.03.015.
- [119] J. Kurzke, H. Ian, *Propulsion and Power: An Exploration of Gas Turbine Performance Modeling*, first ed., Springer, 2018.
- [120] Z. Zhili, L. Kuo, Analysis of heat transfer impacting on gas turbine engine transients, *J. Propuls. Technol.* 17 (3) (1996) 10–15.
- [121] A. Stamatis, K. Mathioudakis, J. Ruiz, B. Curnock, Real Time Engine Model Implementation for Adaptive Control and Performance Monitoring of Large Civil Turbofans, in: Volume 1: Aircraft Engine; Marine; Turbomachinery; Microturbines and Small Turbomachinery, Jun. 2001, vol. 1, pp. 1–7. 10.1115/2001-GT-0362.
- [122] W. Hu, L. Xiaochun, Numerical simulation of effects of heat transfer on the transient performance of gas turbine engines, *J. Propuls. Technol.* 23 (6) (2002) 445–447.
- [123] P.M. Tagade, S.K. Sane, K. Sudhakar, Startup simulation of twin spool turbofan engine, *Int. J. Turbo Jet Engines* 27 (3–4) (Jan. 2010) 265–276, <https://doi.org/10.1515/TJJ.2010.27.3-4.265>.
- [124] M.A. da Cunha Alves, J.R. Barbosa, A step further in gas turbine dynamic simulation, *Proc. Inst. Mech. Eng. Part A J. Power Energy* 217 (6) (Sep. 2003) 583–592, <https://doi.org/10.1177/09565090321700606>.
- [125] C.R. Davison, A.M. Birk, Set Up and Operational Experience With a Micro-Turbine Engine for Research and Education, in: Volume 1: Turbo Expo 2004, Jan. 2004, vol. 1, pp. 849–858. 10.1115/GT2004-53377.
- [126] C.R. Davison, A.M. Birk, Comparison of Transient Modeling Techniques for a Micro Turbine Engine, in: Volume 5: Marine; Microturbines and Small Turbomachinery; Oil and Gas Applications; Structures and Dynamics, Parts A and B, Jan. 2006, no. 6, pp. 449–458. 10.1115/GT2006-91088.
- [127] M. Vieweg, C. Klein, S. Reitenbach, F. Wolters, R.G. Becker, Coupling of predesign and performance tools for transient aircraft engine analyses, 2018.
- [128] A. Ferrand, M. Bellenoue, Y. Bertin, R. Cirligeanu, P. Marconi, F. Mercier-Calvairac, High Fidelity Modeling of the Acceleration of a Turbohaft Engine During a Restart, in: Volume 1: Aircraft Engine; Fans and Blowers; Marine, Jun. 2018, vol. 1, 10.1115/GT2018-76654.
- [129] J.H. Kim, T.S. Kim, Development of a program to simulate the dynamic behavior of heavy-duty gas turbines during the entire start-up operation including very early part, *J. Mech. Sci. Technol.* 33 (9) (Sep. 2019) 4495–4510, <https://doi.org/10.1007/s12206-019-0845-5>.
- [130] Z. Li, Y.G. Li, S. Sampath, Aeroengine transient performance simulation integrated with generic heat soakage and tip clearance model, *Aeronaut. J.* (2022) 1–23, <https://doi.org/10.1017/aer.2022.15>.
- [131] J.A. Kypuros, K.J. Melcher, A reduced model for prediction of thermal and rotational effects on turbine tip clearance, NASA Technical Memorandum, NASA/TM-2003-212226, 2003.
- [132] J.A. Kypuros, R. Colson, A. Muizoz, Improved temperature dynamic model of turbine subcomponents for facilitation of generalized tip clearance control, NASA (2004) NAG3-2857.
- [133] P. Pilidis, N.R.L. MacCallum, A Study of the Prediction of Tip and Seal Clearances and Their Effects in Gas Turbine Transients, in: Volume 1: Turbomachinery, Jun. 1984, vol. 106, no. December 1984, 10.1115/84-GT-245.
- [134] N.R.L. MacCallum, Transient Expansion of the Components of an Air Seal on a Gas Turbine Disc, Feb. 1977, 10.4271/770974.
- [135] J.L. Kratz, J.W. Chapman, Active Turbine Tip Clearance Control Trade Space Analysis of an Advanced Geared Turbofan Engine, Jul. 2018, 10.2514/6.2018-4822.
- [136] H. Sheng, T. Liu, Y. Zhao, Q. Chen, B. Yin, R. Huang, New model-based method for aero-engine turbine blade tip clearance measurement, *Chinese J. Aeronaut.* no. September (Sep. 2022), <https://doi.org/10.1016/j.cja.2022.09.012>.
- [137] Y. Fang, Y. Liu, Y. Yu, X. He, Radial displacement of HPT rotor caused by the centrifugal and heat, *Gas Turbine Exp. Res.* 24 (2) (2011) 31–35, <https://doi.org/10.3969/j.issn.1627-9730.2011.02.051>.
- [138] Y. Fang, Y. Liu, X. He, Study of the radial elongations of the turbine rotor with the centrifugal effect, *Sh. Electron. Eng.* 31 (2) (2011) 9–12, <https://doi.org/10.3969/j.issn.1627-9730.2011.02.051>.
- [139] G.A. Halls, Air cooling of turbine blades and vanes, *Aircr. Eng. Aerosp. Technol.* 39 (8) (Aug. 1967) 4–14, <https://doi.org/10.1108/eb034284>.
- [140] B. Lakshminarayana, Methods of predicting the tip clearance effects in axial flow turbomachinery, *J. Basic Eng.* 92 (3) (Sep. 1970) 467–480, <https://doi.org/10.1115/1.3425036>.
- [141] E.A. Basakharone, *Principles of Turbomachinery in Air-Breathing Engines*, Cambridge University Press, 2006.
- [142] H. Chen, Z. Zhili, The investigation of the simulating model for transient performance of the turbofan engine, *J. Aerosp. Power* 17(2) (2002) 75–79. 10.13224/j.cnki.jasp.2002.01.013.
- [143] W. Jiamei, X. Xuan, T. Qiuye, Z. Kang, Y. Kun, The effects of tip clearance of compressors on the engine transient, 2019.
- [144] X. Ma, *Heat soakage Effects on Gas Turbine Engine Performance*, Cranfield University, 2021. MSC thesis.
- [145] A.G. Hourmouziadis J., An Integrated Aero/Mechanical Performance Approach to High Technology Turbine Design, AGARD, 1987, <https://www.sto.nato.int/publications/AGARD/AGARD-CP-421/AGARD-CP-421.pdf> (accessed 14 March 2023).
- [146] M.R. Shirzadi, H. Saeidi, The Effects of Tip Clearance on Performance of a Heavy Duty Multi Stages Axial Turbine, in: Volume 8: Turbomachinery, Parts A, B, and C, Jun. 2012, vol. 8, no. PARTS A, B, AND C, pp. 1531–1541, 10.1115/GT2012-69553.
- [147] N.R.L. MacCallum, Thermal Influences in Gas Turbine Transients: Effects of Changes in Compressor Characteristics, Mar. 1979, 10.1115/79-GT-143.
- [148] N.R.L. MacCallum, Effect of ‘Bull’ Heat Transfers in Aircraft Gas Turbines on Compressor Surge Margins, 1973, [https://www.scopus.com/record/display.uri?eid=2-s2.0-85042249153&origin=resultslist&sort=r-f&src=s&id=4335a063ca0ba22ba29818a52c94fa0f&sort=aut&sdt=a&sl=17&s=AU-ID%286701497875%29&relpos=9&citeCnt=0&searchTerm=">https://www.scopus.com/record/display.uri?eid=2-s2.0-85042249153&origin=resultslist&sort=r-f&src=s&id=4335a063ca0ba22ba29818a52c94fa0f&sort=aut&sdt=a&sl=17&s=AU-ID%286701497875%29&relpos=9&citeCnt=0&searchTerm="> \(accessed 14 March 2023\).](https://www.scopus.com/record/display.uri?eid=2-s2.0-85042249153&origin=resultslist&sort=r-f&src=s&id=4335a063ca0ba22ba29818a52c94fa0f&sort=aut&sdt=a&sl=17&s=AU-ID%286701497875%29&relpos=9&citeCnt=0&searchTerm=)
- [149] A.D. Grant, *The Effect of Heat transfer on boundary layer stability*, University of Glasgow, 1973. PhD thesis.
- [150] N.R.L. MacCallum, A.D. Grant, The Effect of Boundary Layer Changes Due to Transient Heat Transfer on the Performance of an Axial-Flow Air Compressor, in: SAE Technical Papers, Feb. 1977, pp. 1357–1364, 10.4271/770284.
- [151] R. Crawford, A. Burwell, Quantitative evaluation of transient heat transfer on axial flow compressor stability, Jul. 1985, 10.2514/6.1985-1352.
- [152] N.R.L. MacCallum, Further Studies of the Influence of Thermal Effects on the Predicted Acceleration of Gas Turbines, in: Volume 1: Aircraft Engine; Marine; Turbomachinery; Microturbines and Small Turbomachinery, Mar. 1981, no. 81-GT-21, pp. 1–8, 10.1115/81-GT-21.
- [153] P. Pilidis, N.R.L. MacCallum, A General Program for the Prediction of the Transient Performance of Gas Turbines, Mar. 1985, 10.1115/85-GT-209.
- [154] N.R.L. MacCallum, P. Pilidis, The Prediction of Surge Margins During Gas Turbine Transients, Mar. 1985, 10.1115/85-GT-208.
- [155] A.G. Stamatis, K. Mathioudakis, The Influence of Heat Transfer Effects on Turbine Performance Characteristics, in: Volume 3: Heat Transfer, Parts A and B, Jan. 2006, vol. 3 PART A, pp. 829–838, 10.1115/GT2006-91039.
- [156] J. Larjola, Simulation of Surge Margin Changes due to Heat Transfer Effects in Gas Turbine Transients, in: Volume 2: Aircraft Engine; Marine; Microturbines and Small Turbomachinery, Jun. 1984, vol. 1, pp. 1–9, 10.1115/84-GT-129.
- [157] G. Torella, Transient performance and behaviour of gas turbine engines, Proc. ASME Turbo Expo 2 (1990), <https://doi.org/10.1115/90-GT-188>.
- [158] M. Morini, G. Cataldi, M. Pinelli, M. Venturini, A Model for the Simulation of Large-Size Single-Shaft Gas Turbine Start-Up Based on Operating Data Fitting, in: Volume 6: Turbo Expo 2007, Parts A and B, Jan. 2007, vol. 6 PART B, pp. 1849–1856, 10.1115/GT2007-27373.
- [159] P.N. Shah, *“Novel Turbomachinery Concepts for Highly Integrated Airframe / Propulsion Systems*, Massachusetts Institute of Technology, 2007. PhD thesis.

- [160] A. Kiss, Z. Spakovszky, Effects of Transient Heat Transfer on Compressor Stability, in: Volume 1: Aircraft Engine; Fans and Blowers; Marine, Jun. 2018, vol. 140, no. 12, pp. 1–11. 10.1115/GT2018-75413.
- [161] A. Kiss, Z. Spakovszky, Effects of transient heat transfer on compressor stability, *J. Turbomach.* 140 (12) (Dec. 2018) 1–9, <https://doi.org/10.1115/1.4041290>.
- [162] Z.-J. Li, Y.-G. Li, T. Korakianitis, Gas Turbine Transient Performance Simulation With Simplified Heat Soakage Model, in: Volume 5: Controls, Diagnostics, and Instrumentation; Cycle Innovations; Cycle Innovations: Energy Storage, Sep. 2020, vol. 5, no. 1968, pp. 1–12, 10.1115/GT2020-14484.
- [163] L. Ming et al., Influence of the tip and axial clearances on the aerodynamic performance of a helium compressor, *Qinghua Daxue Xuebao/J. Tsinghua Univ.*, 57(8) (2017) 832–837, 10.16511/j.cnki.qhdxxb.2017.22.046.
- [164] A. Grönman, T. Turunen-Saaresti, P. Röyttä, A. Jaatinen-Väri, Influence of the axial turbine design parameters on the stator–rotor axial clearance losses, *Proc. Inst. Mech. Eng. Part A J. Power Energy* 228 (5) (Aug. 2014) 482–490, <https://doi.org/10.1177/0957650914531949>.

Gas turbine engine transient performance and heat transfer effect modelling: a comprehensive review, research challenges, and exploring the future

Yang, Yimin

2023-09-12

Attribution 4.0 International

Yang Y, Nikolaidis T, Jafari S, Pilidis P. (2024) Gas turbine engine transient performance and heat transfer effect modelling: a comprehensive review, research challenges, and exploring the future. Applied Thermal Engineering, Volume 236, Part A, Article number 121523

<https://doi.org/10.1016/j.applthermaleng.2023.121523>

Downloaded from CERES Research Repository, Cranfield University